



## Molecular mechanisms of the chemical constituents from anti-inflammatory and antioxidant active fractions of *Ganoderma neo-japonicum* Imazeki

Rui-rui Zhang<sup>a,b,1</sup>, Jing Zhang<sup>b,1</sup>, Xu Guo<sup>b</sup>, Ying-ying Chen<sup>b</sup>, Jin-yue Sun<sup>b</sup>, Jia-lin Miao<sup>d</sup>, M. Carpena<sup>e</sup>, M.A. Prieto<sup>e,f,\*</sup>, Ning-yang Li<sup>c,\*\*</sup>, Qing-xin Zhou<sup>a,b,\*\*\*</sup>, Chao Liu<sup>b,d,\*\*\*\*</sup>

<sup>a</sup> Institute of Biomedical Sciences, College of Life Sciences, Key Laboratory of Animal Resistance Biology of Shandong Province, Shandong Normal University, Jinan, Shandong, PR China

<sup>b</sup> Key Laboratory of Novel Food Resources Processing, Ministry of Agriculture and Rural Affairs, Key Laboratory of Agro-Products Processing Technology of Shandong Province, Institute of Agro-Food Science and Technology, Shandong Academy of Agricultural Sciences, 202 Gongye North Road, Jinan, 250100, PR China

<sup>c</sup> College Food Science and Engineering, Shandong Agricultural University, Tai An, 271018, Shandong, PR China

<sup>d</sup> Weihai Yuwang Group CO., LTD, Wei Hai, 264209, Shandong, PR China

<sup>e</sup> Universidade de Vigo, Nutrition and Bromatology Group, Department of Analytical Chemistry and Food Science, Faculty of Science, E32004, Ourense, Spain

<sup>f</sup> Agrifood Research Group, Galicia Sur Health Research Institute (IIS Galicia Sur). SERGAS-UVIGO, Spain

### ARTICLE INFO

Handling Editor: A.G. Marangoni

#### Keywords:

*Ganoderma neo-japonicum* Imazeki  
LC-MS/MS  
Triterpenoids  
Antioxidant ability  
Anti-inflammatory activity

### ABSTRACT

*Ganoderma neo-japonicum* Imazeki is a rare medicinal mushroom that has been reported to play a role in scavenging free radicals, protecting the liver, and inhibiting tumor cell activity. In this study, crude extracts were prepared, and 47 triterpenoids were identified by Ultra-high-performance liquid chromatography coupled with triple quadrupole time-of flight mass spectrometry (UHPLC-Triple TOF-MS/MS). Then, the crude extracts were subjected to column chromatography for the first time to obtain six fractions (Fr. (a), (b), (c), (d), (e) and (f)). Antioxidant and anti-inflammatory active tracking assays of all fractions found that Fr. (c) exhibited the strongest bioactivity. Subsequently, the chemical composition of Fr. (c) was clarified, and eight triterpenoids were determined in combination with the standard substances. In addition, this study demonstrated that Fr. (c) reduced the levels of inflammatory cytokines and reactive oxygen species (ROS) in LPS-stimulated RAW264.7 macrophages. Further studies showed that Fr. (c) could down-regulate the expression level of proteins associated of NF- $\kappa$ B signaling pathway, and upregulated Nrf2 and HO-1 protein level. In conclusion, our study showed that Fr. (c) inhibited LPS-mediated inflammatory response and oxidative stress by activating the Nrf2/HO-1 pathway and inactivating the NF- $\kappa$ B pathway. In the future, with the clearing of its composition and activity mechanism, Fr. (c) of *G. neo-japonicum* are expected to become a functional food for health and longevity.

### 1. Introduction

The genus *Ganoderma* is taxonomically classified, hierarchically from

specific to general, into the Basidiomycota division, Agaricomycetes class, Polyporales order, and finally, Ganodermataceae family (Zeng et al., 2017). At present, there are 131 species of *Ganoderma* worldwide, among which approximately 70 species are widely distributed in China,

\* Corresponding authors. Universidade de Vigo, Nutrition and Bromatology Group, Department of Analytical Chemistry and Food Science, Faculty of Science, E32004, Ourense, Spain.

\*\* Corresponding author.

\*\*\* Corresponding authors. Institute of Biomedical Sciences, College of Life Sciences, Key Laboratory of Animal Resistance Biology of Shandong Province, Shandong Normal University, Jinan, Shandong, PR China.

\*\*\*\* Corresponding author. Key Laboratory of Novel Food Resources Processing, Ministry of Agriculture and Rural Affairs, Key Laboratory of Agro-Products Processing Technology of Shandong Province, Institute of Agro-Food Science and Technology, Shandong Academy of Agricultural Sciences, 202 Gongye North Road, Jinan, 250100, PR China.

E-mail addresses: [mprieto@uvigo.es](mailto:mprieto@uvigo.es) (M.A. Prieto), [ningyangli@126.com](mailto:ningyangli@126.com) (N.-y. Li), [zhouqx0211@163.com](mailto:zhouqx0211@163.com) (Q.-x. Zhou), [liuchao555@126.com](mailto:liuchao555@126.com) (C. Liu).

<sup>1</sup> These authors contributed equally to this work.

<https://doi.org/10.1016/j.crfs.2023.100441>

Received 9 November 2022; Received in revised form 23 December 2022; Accepted 10 January 2023

Available online 25 January 2023

2665-9271/© 2023 Published by Elsevier B.V. This is an open access article under the CC BY-NC-ND license (<http://creativecommons.org/licenses/by-nc-nd/4.0/>).

## Abbreviations

### List of generic abbreviations

TCM	Traditional Chinese Medicine
ROS	Reactive Oxygen Species
SOD	Superoxide Dismutase
CH <sub>2</sub> Cl <sub>2</sub>	Dichloromethane
CC	Column Chromatography
Vc	Vitamin C
FBS	Fetal Bovine Serum
OD	Optical Density
DMSO	dimethyl sulfoxide
LPS	Lipopolysaccharide
DXM	Dexamethasone
DMEM	Dulbecco's Modified Eagle's Medium
FBS	Fetal Bovine Serum
NO	Nitric Oxide
TIC	Total Ion Current
IL	Interleukin
iNOS	Nitric Oxide Synthase
Keap1	Kelch-Like ECH-Associated Protein 1
HO-1	Heme Oxygenase 1

Japan, and the Korean Peninsula (Ma et al., 2014; Xing et al., 2018). There are many traditional appellations of *Ganoderma* species, such as “Ling-zhi-cao”, “Rui-cao”, “Xian-cao” or “Wan-nian-rong” in China and “Rei-shi” in Japan, because of their effectiveness. In 2012, Cao et al., proposed that the East Asian *Ganoderma* species could be a new fungal taxon different from the European species and was given the name *Ganoderma lucidum*, also known as “Lingzhi” (Cao et al., 2012).

As a functional medicine and food for the amelioration of health and longevity, *Ganoderma* species have been used in Traditional Chinese Medicine (TCM) for more than two millennia (Fu et al., 2019; Leskossek-Cukalovic et al., 2010). *Ganoderma* species are considered legal crude drug medicines in the Chinese Pharmacopoeia (2015 edition) for preventing cancer, neurodegeneration, and cardiovascular diseases in the clinic stage (Chung et al., 2017; González et al., 2020). In addition, modern pharmacological and clinical investigations have also demonstrated that *Ganoderma* species have various pharmacological effects and biological activities such as antioxidant, anti-inflammatory, anti-aging, antitumor, and hepatoprotective, and other medicinal activities. (Fujita et al., 2005; Martínez-Montemayor et al., 2019). The main bioactive compounds include triterpenoids, polysaccharides, sterols, and proteins extracted from its fruiting bodies (basidiocarps), which are responsible for these biological activities of *Ganoderma* species (Chung et al., 2017; González et al., 2020). Among them, triterpenes are one of the main active components of *Ganoderma lucidum*, which inhibit various inflammatory reactions *in vivo* (Feng and Wang, 2019; C. Liu et al., 2015; Wu et al., 2019). Based on the reported anti-inflammatory activities of *G. lucidum* triterpenes, they mainly inhibited the release of pro-inflammatory cytokines such as TNF- $\alpha$ , IL-2, PGE<sub>2</sub>, etc., partly related to blocking the activation of NF- $\kappa$ B pathway and TLR4 expression (Dudhgaonkar et al., 2009; Wu et al., 2019). In addition, some *Ganoderma* triterpenes exert anti-inflammatory effects by blocking the phosphorylation of p38 to inhibit the MAPK pathway (Su et al., 2020; Xu et al., 2021). Recent studies have proved that *Ganoderma lucidum* triterpenoids can also play a pharmacological role in the peripheral and central nervous system, alleviate anxiety and depression like behavior of mice by reducing inflammation (Mi et al., 2022), and reduce neuronal apoptosis and neuro-inflammation in Alzheimer's disease mice (Yu et al., 2020; Y. Zhang et al., 2021).

In biological systems, free radicals and reactive oxygen species (ROS) are constantly produced as metabolic by-products in biological systems.

When the body lacks antioxidant defense, a large number of free radicals and ROS lead to oxidative stress reactions (E. Obrenovich et al., 2012; Maheshwari et al., 2022). *G. lucidum* has strong antioxidant activity, and its active ingredients can enhance the activities of superoxide dismutase (SOD) and catalase, thereby reducing the level of ROS (Ajith et al., 2009; Smina, De, et al., 2011). Zhu et al. studied that the lanostanoid triterpenes obtained from the *Ganoderma* family not only have neuro-protective effects, but also scavenge free radicals and reduce oxidative damage (Chen et al., 2018; Qiu et al., 2016). Recent studies have shown that FYGL, a proteoglycan extracted from *G. lucidum*, has significant antioxidant activity and protects pancreatic  $\beta$  cells from apoptosis caused by oxidative stress by inhibiting MAPK and NF- $\kappa$ B signaling pathways (Pan et al., 2022).

*G. neo-japonicum* Imazeki is an annual saprophytic fungus that grows in decaying tropical bamboo bushes. As a precious medicinal fungus, *G. neo-japonicum* Imazeki is grown in many Asian countries. In Malaysia, residents use the fungus as an herbal remedy for various diseases and cancers. The morphological characteristics of *G. neo-japonicum* are relatively like those of *G. sinensis*, except *G. neo-japonicum* has a semi-circular cap and kidney rows, and the color is reddish brown or purple reddish brown. In China, it can be used as a healthy food and, in 2018, the National Health Commission of China proposed the administration of *Ganoderma* species as ordinary food substances in some areas (State Health Office Food Letter No. 2018278), and Shandong Province is the pilot province for the promotion of *G. lucidum* food. One of the earliest studies showed that water extract of *G. neo-japonicum* has the effect of scavenging free radicals, and has a protective effect on CCl<sub>4</sub>-induced liver injury in rats (Lin et al., 1995). In addition to this, water extract of *G. neo-japonicum* promotes neurogenesis by activating MEK/ERK1/2 and PI3K/Akt signaling pathways (Ling-Sing Seow et al., 2013). The green silver nanoparticles (AgNPs) synthesized from *G. neo-japonicum* extract exert an anti-breast cancer effect (Gurunathan et al., 2013). The wheat grains fermented by *G. neo-japonicum* mycelia have better antioxidant and adipogenesis activities, and could modulate PPAR $\gamma$  expression in 3T3-L1 cells (Subramaniam et al., 2015). Recent studies have found that *G. neo-japonicum* has inhibitory activity on human colon cancer cells (Lau et al., 2022).

Although crude extracts of *G. neo-japonicum* have been verified to have obvious antioxidant and anti-inflammatory effects, the specific active fractions, mainly chemical components, and related molecular mechanisms, have not been studied. Therefore, crude extracts containing the total triterpene content of *G. neo-japonicum* were prepared and subjected to column chromatography (CC) for the first time to obtain different fractions, and the antioxidant and anti-inflammatory activities of all fractions were evaluated in this study. Subsequently, the chemical constituents of the crude extracts and the most active fractions were identified and analyzed by HPLC-DAD-Triple-TOF/MS. In addition, the effects and relevant molecular mechanism of the most active fractions on the release of inflammatory factors and inflammation-related pathways in LPS-induced RAW264.7 cells were also investigated.

## 2. Materials and methods

### 2.1. Chemicals and reagents

The fruiting bodies of *G. neo-japonicum* were obtained in May 2019 from Guan County of Shandong province, China. The voucher specimen was identified by Prof. Jin-Yue Sun, Shandong Academy of Agricultural Sciences, Jinan, China, and was deposited at the Natural Pharmacy Laboratory of the SAAS, Jinan, China under the reference (No. 20190514). The chemicals perchloric acid, vanillin, and glacial acetic acid were purchased from Sinopharm Chemical Reagent Co., Ltd. (Shanghai, China). The analytical grade solvents used in this experiment, including methanol, ethanol, acetonitrile, and phosphoric acid, were acquired from J & K Chemical Ltd. (Beijing, China). Triterpenoid standard substances, including Ganolucidic acid F ( $\geq 98.0\%$ ),

Ganodermanontriol ( $\geq 98.0\%$ ), Ganoderal A ( $\geq 98.0\%$ ), Ganoderenic acid B ( $\geq 98.0\%$ ), Ganoderiol D (97.0%), and Oleanolic acid ( $\geq 98.0\%$ ), were bought from Chengdu Alfa Biotechnology Co., Ltd. (Sichuan, China). Lucidenic acid L (98.0%), and Ganoderic acid S (97.5%) were gained from Sichuan Weikeqi Biological Technology Co., Ltd. (Sichuan, China) and Shanghai Yuanye Biological Technology Co., Ltd. (Shanghai, China), respectively. Ganoderic acid beta (95.4%) were prepared by us. These compounds were identified through LC-MS/MS and database comparison. Before the experiment, all samples were filtered through 0.45  $\mu\text{m}$  filter membrane.

Both the 2,2-diphenyl-1-picrylhydrazyl (DPPH), ascorbic acid (vitamin C; Vc), dimethyl sulfoxide (DMSO), lipopolysaccharide (LPS), and dexamethasone (DXM) were obtained from Sigma-Aldrich (Saint Louis, MO, USA). Dulbecco's modified Eagle's medium (DMEM), penicillin/streptomycin and fetal bovine serum (FBS) were obtained from Gibco (New York, NY, USA). The ABTS kit, FRAP kit, nitric oxide (NO) assay kit and CCK-8 kit was purchased from Beyotime Biotechnology Co., Ltd. (Jiangsu, China). ELISA Kits for mouse PGE2, TNF- $\alpha$ , IL-1 $\beta$  and IL-6 were purchased from R&D systems (Minneapolis, MN, USA). The anti-iNOS, anti-LaminB, anti-Nrf2, anti-HO-1 and anti-NF- $\kappa\text{B}$  were obtained from Abcam (Cambridge, MA, USA). The anti-phospho-NF- $\kappa\text{B}$ , anti-I $\kappa\text{B}\alpha$ , anti-phospho-I $\kappa\text{B}\alpha$ , anti-COX-2, and anti- $\beta$ -actin were obtained from Cell Signaling Technology (Danvers, MA, USA). The related secondary antibodies and anti-Keap1 were purchased from Proteintech Technology Co. Ltd. (Hubei, China).

## 2.2. Preparation of the crude extracts and compound from the fruiting bodies of *G. neo-japonicum*

The fruiting bodies of *G. neo-japonicum* Imazeki were air-dried at 28 °C nearly 3 days after rinsing in the natural environment until the final moisture content lower 4% and then pulverized by a laboratory crusher. Subsequently, the crushed *G. neo-japonicum* was passed through an 80-mesh screen to obtain the powder. The powder (3.5 kg) was extracted with 50% ethanol (70 L) by heating at 50 °C for 4 h using a Chemical reaction kettle, and then the mixture was filtered to obtain the extracted solution. The extracted solution was concentrated by rotary evaporation (Gongyi City Yuhua Instrument Co., Ltd., Henan, China) to obtain the crude extracts (104 g). The crude extracts were dissolved in deionized water (3.5 L) and extracted with the same volume of dichloromethane ( $\text{CH}_2\text{Cl}_2$ ) (Shizhong Zheng et al., 2020). The  $\text{CH}_2\text{Cl}_2$  layer was taken after layering and then concentrated under pressure to obtain the final extracts containing the total triterpene content (28.92 g). Then, it was passed through a silica gel column and eluted with a petroleum ether-ethyl acetate (1:0-2:1, 1500 mL each) gradient to obtain six fractions based on the Thin-layer chromatography (TLC) analysis: Fr. (a) 3.49 g (1:0-10:1), (b) 1.03 g (10:1-8:1), (c) 7.625 g (8:1-6:1), (d) 8.18 g (6:1-4:1), (e) 1.73 g (4:1-3:1), (f) 1.045 g (3:1-2:1).

Then, Fr. (c) was firstly separated by CC over silica gel, eluted with various petroleum ether-acetone gradients (50:1~1:2, 1.0 L each) to yield 5 subfractions with TLC tracing: Fr. (1) 1.01 g (50:1-15:1), (2) 0.74 g (15:1-10:1), (3) 0.20 g (10:1-8:1), (4) 0.72 g (7:1-1:1) and (5) 0.82 g (1:1-1:2). Fr. (3) (petroleum ether-acetone 10:1-8:1, ca. 0.2 g) was purified by semi-preparative HPLC with gradient elution 65–100% MeOH/H<sub>2</sub>O (2 mL/min, 30 min) following another 100% MeOH (2 mL/min, 10 min) as the isocratic solvent system to yield Ganoderic acid beta (3.1 mg, tR 17.106 min). Purity of it (95.4%) was determined by HPLC eluted with 80% MeOH/H<sub>2</sub>O containing 0.1% glacial acetic acid at a flow rate of 1 mL/min. The separated flow chart is shown in Fig. S1.

## 2.3. UHPLC-triple TOF-MS/MS and HPLC analysis

The stock solution of the triterpenoids was obtained by dissolving each standard substance in methanol at a concentration of 1 mg/mL and kept at 4 °C. The standard working solution was obtained by diluting the stock solution with methanol before its use (X. D. Zhang et al., 2016).

An Agilent 1260 UHPLC (Agilent Technologies USA) connected to a reversed-phase column (250  $\times$  4.6 mm i.d., 5  $\mu\text{m}$ , Agilent, USA) was used to analyze the components of the crude extract, and Fr. (c) for crude extracts. The mobile phase was composed of 0.3% glacial acetic acid in aqueous solution (A) and acetonitrile (B). The gradient of the mobile phase was as follows: 0–5 min, 10–28% B, 5–15 min, 28–50% B; 15–35 min, 50–80% B, 35–55 min, 80–95% B, 55–65 min, 95–100% B. The column temperature was maintained at 35 °C, and the flow rate was set at 0.8 mL/min. The detection wavelength was 250 nm, and the injection volume was set as 10  $\mu\text{L}$ . For Fr. (c), the mobile phase consisted of 0.1% formic acid in water (A) and 0.03% formic acid in acetonitrile (C). The mobile phase was carried out with an elution gradient as follows: 0 min, 10% C; 5 min, 35% C; 15 min, 50% C; 35 min, 80% C; 55 min, 100% C; 60 min, 100% C, and the flow rate was set at 0.8 mL/min. The injection volume was 5  $\mu\text{L}$ . Absorption values were determined at 250 nm. Raw spectra were imported using Progenesis QI software.

A Nexera Triple-TOF/MS system (Nexera, Japan) equipped with an ESI ion source (AB Sciex, USA) was applied to identify the triterpenoids in positive (+) ion mode. In addition, a Triple-TOF/MS can perform primary and secondary mass spectral data collection based on the IDA function under the control of the software (Analyst TF 1.7, AB Sciex). The source parameters were as follows: nebulizer gas (GS1; GS2): 55 psi; bombardment energy: 40 eV; poor collision energy: 20 V; electrospray capillary voltage (IS): 5500 V; source temperature (TEM): 550 °C. The mass spectrometric data were gathered in the range of 100–1500  $m/z$  in positive ion centroid mode.

## 2.4. Determination of total triterpene content

The determination of the total triterpene content was performed as described by Wei et al. (2018) with minor modifications. Oleanolic acid was used as the standard curve. Firstly, the crude extracts (20 mg) were dissolved in 4 mL of methanol (100%) to obtain the sample solution (5 mg/mL). Sample solutions (50  $\mu\text{L}$ ) were sequentially added to 75  $\mu\text{L}$  of vanillin-glacial acetic acid solution (5%) and 250  $\mu\text{L}$  of perchloric acid solution and then reacted in a 60 °C water-bath for 45 min followed by an ice bath. Subsequently, glacial acetic acid (1.125 mL) was added for quantification, and the absorbance of the above reaction solution was measured at 550 nm. The determination of the standard curve was performed according to the above steps. All samples were analyzed in triplicate and the extraction rate of total triterpenes from *G. neo-japonicum* was calculated as described by Eq. [1]:

$$Y (\text{mg/g}) = \frac{C \times V}{M} \quad (1)$$

where Y: total triterpenoid extraction rate (mg/g); C: the concentration of the target compound in the sample solution (mg/mL); V: the sample solution volume (mL); M: the dry weight of *G. neo-japonicum* (mg).

## 2.5. Determination of antioxidant capacity in vitro

The antioxidant activities of the six fractions Fr. (a), (b), (c), (d), (e) and (f), and crude extracts were evaluated at seven different initial concentrations (0.1 mg/mL, 0.2 mg/mL, 0.4 mg/mL, 0.6 mg/mL, 0.8 mg/mL, 1 mg/mL, and 2 mg/mL), and diluted differently depending on the different antioxidant experiments.

### 2.5.1. DPPH radical scavenging assay

DPPH (2,2-Diphenyl-1-picrylhydrazyl) is a stable free radical that can be used to measure the free radical scavenging activity of antioxidants. Different concentrations of sample solutions (20  $\mu\text{L}$ ) were mixed with DPPH methanol solution (180  $\mu\text{L}$ ; 0.04 mg/mL) in 96-well plates. After 30 min incubation at room temperature in the dark, absorbance was measured at 515 nm. Methanol was used as negative control and vitamin C (Vc) was used as a positive control. The scavenging activity of

each sample was calculated according to Eq. [2]:

$$Y = \left(1 - \frac{A_{\text{sample}}}{A_{\text{control}}}\right) \times 100\% \quad (2)$$

where  $Y$  is scavenging activity;  $A_{\text{control}}$  is the absorbance of the negative control and  $A_{\text{sample}}$  is the absorbance of the ethanol solution of DPPH with the tested sample.

### 2.5.2. Scavenging activity on ABTS radical

The ABTS (2,2'-azino-bis (3-ethylbenzothiazoline-6-sulfonic acid)) free radical decolorization assay was used to measure the total antioxidant activity of the samples. The prepared ABTS stock solution was stored at room temperature for 16 h in the dark. Before used, it was diluted with ethanol (95%) and absorbance was measured at 734 nm to obtain working solution. Subsequently, ABTS working solution (200  $\mu\text{L}$ ) was mixed with different concentrations of sample solutions (10  $\mu\text{L}$ ), incubated at room temperature for 6 min, and the absorbance was measured at 734 nm. All experiments were performed in triplicate.

The scavenging activity was plotted against different concentrations of 6-hydroxy-2,5,7,8-tetramethylchroman-2-carboxylic acid (Trolox) to acquire the regression equation and to calculate the value of the sample solution.

### 2.5.3. FRAP assay

The FRAP (Ferric reducing ability of plasma) assay was performed according to the method of Lachowicz et al. (2020) with minor modifications. Briefly, freshly prepared working solutions were incubated at 37 °C for 30 min before use. FRAP working solution (180  $\mu\text{L}$ ) was mixed with sample solutions of different concentrations and incubated for 15 min in a 37 °C water bath. When the  $\text{Fe}^{3+}$ -TPTZ complex is reduced to  $\text{Fe}^{2+}$ , a blue complex is formed. Then, the absorbance was measured at 593 nm. All the experiments were performed in triplicate. The standard curve was prepared using  $\text{FeSO}_4$  ranging from 0.15 mmol/L to 1.5 mmol/L. The results are expressed as  $\text{FeSO}_4$  equivalents mmol/L.

## 2.6. Anti-inflammatory assay

### 2.6.1. Cell culture

The RAW264.7 mouse macrophage cell line was purchased from American Type Culture Collection (ATCC, USA) and grown in DMEM/high glucose medium containing 10% FBS and penicillin/streptomycin in a humidified incubator with 5%  $\text{CO}_2$  at 37 °C.

### 2.6.2. Cell viability

CCK-8 assay was used to determine the effect of the extracts on cell cytotoxicity. RAW264.7 cells in logarithmic growth phase were inoculated in 96-well plates at a density of  $2 \times 10^4$  cells/well (100  $\mu\text{L}$ ). After 12 h, the plating medium was replaced with fresh medium containing *Ganoderma* samples of different concentrations (0–100  $\mu\text{g}/\text{mL}$ ). After 24 h, 10  $\mu\text{L}$  of the CCK-8 solution was added to the culture media, and the plate was incubated at 37 °C for 2 h. Subsequently, the optical density (OD) was measured with a microplate reader (BioRad, Hercules, CA, USA) at 450 nm.

### 2.6.3. Evaluation of nitric oxide (NO) production

RAW264.7 cells were seeded in 96-well plates at a density of  $2 \times 10^4$  cells/mL and were cultured for 12 h. The cells were pretreated with different concentrations of *Ganoderma* sample for 2 h. After 2 h, LPS (1  $\mu\text{g}/\text{mL}$ ) was cotreated with the cells for 18 h to induce an inflammatory response. Then, the production of NO in the medium was measured using Griess reagent kit (Beyotime, Shanghai, China). Briefly, 100  $\mu\text{L}$  of Griess reagent was mixed with 100  $\mu\text{L}$  of the cell-free supernatants and incubated at room temperature for 10 min. The absorbance was measured at 540 nm against a standard sodium nitrite curve using a microplate reader (BioRad, Hercules, CA, USA).

**Table 1**

Primer sequences used in this study for qRT-PCR amplification.

Gene	Forward primer (5'-3')	Reverse primer (5'-3')
IL-1 $\beta$	GTCITTCGCCGTGGACCTTC	GTCITTCGCCGTGGACCTTC
IL-6	TTGCCCTTCTGGGACTGAT	TTGCCATTGCACAACCTCTT
TNF- $\alpha$	TCTCATTCCTGCTTGTTGGC	CACITGGTGGTTTGCTACG
$\beta$ -actin	TCGTGCGTGACATCAAAGA	ATGCCACAGGATTCATACC

### 2.6.4. ELISA assay

RAW264.7 cells in logarithmic growth phase were seeded in 12-well plates at a density of  $1 \times 10^6$  cells/well for 12 h. The cells were pretreated with different concentrations of Fr (c) for 2 h and then co-treated with LPS (1  $\mu\text{g}/\text{mL}$ ) for 24 h to induce an inflammatory response. The cell supernatants were harvested, and the production levels of PGE2, TNF- $\alpha$ , IL-1 $\beta$  and IL-6 were determined by ELISA kit according to the manufacturer's instructions.

### 2.6.5. RNA extraction and real-time PCR analysis

RAW 264.7 cells were treated with 1  $\mu\text{g}/\text{mL}$  LPS in the presence or absence of Fr (c) (6.25, 12.5, and 25  $\mu\text{g}/\text{mL}$ ). After treatment, total RNA was extracted using TRIzol reagent (Invitrogen, CA, USA), and reverse transcribed into cDNA using a reverse transcription kit (Vazyme, Nanjing, China). The RT-qPCR reaction system was prepared using SYBR® Green Premix ExTaq II (TLiRNaseH Plus) (Thermo Fisher, Dreieich, Germany) according to the manufacturer's instructions, and the procedure was performed using an ABI 7500 qPCR system (Life Technologies). According to the amplification curve data, the final data were analyzed using the comparative Ct method ( $2^{-\Delta\Delta\text{Ct}}$ ). The primers were synthesized by TSINGKE Biological Technology (Beijing, China). Actin expression was used as an endogenous control. The primer sequences used in the study are shown in Table 1.

### 2.6.6. ROS level evaluation

Intracellular ROS accumulation was monitored with the ROS Assay Kit (Beyotime, Shanghai, China). After the cells were treated as described above, 10  $\mu\text{M}$  of 2',7'-dichlorofluorescein diacetate (DCFH-DA) was added, and the cells were incubated in a 37 °C cell incubator for 20 min. Cells were washed three times with serum-free cell culture medium, and then the level of ROS was measured by flow cytometry and Leica fluorescence microscope.

### 2.6.7. Western blot

RAW264.7 cells were treated with 1  $\mu\text{g}/\text{mL}$  LPS alone or with different concentrations of Fr (c) (6.25, 12.5, 25  $\mu\text{g}/\text{mL}$ ) as previously describe. After treatment, total proteins were extracted using RIPA lysis buffer, and the protein concentration was quantified with a BCA kit (Beyotime, Shanghai, China). Protein (60  $\mu\text{g}/\text{well}$ ) was separated by 10% or 12% SDS-PAGE and transferred to PVDF membranes. The PVDF membrane was blocked with 5% nonfat milk on a shaker at room temperature for 1 h, then incubated with primary antibodies at 4 °C for overnight. The PVDF membrane was washed three times with TBST and then incubated with the HRP-conjugated Affinipure Goat Anti-Rabbit IgG(H + L) or HRP-conjugated Affinipure Goat Anti-Mouse IgG(H + L) secondary antibodies for 2 h at room temperature. The blots were washed with TBST three times and visualized with an enhanced ECL detection kit. The results were analyzed using ImageJ software (NIH, Bethesda, MD, USA).

## 2.7. Molecular docking

In this study, the VINA 1.1.2 software was used to conduct docking research on the interactions compound-protein of the extracts to bind the 1X2R region of Keap1 and the 1IKN region of NF- $\kappa\text{B}$ . The binding energy was reduced from 6.0 kcal/mol to 5.0 kcal/mol, indicating that the compound could spontaneously bind well to the protein. Then,

**Table 2**

The component identification results of the crude extracts from *G. neo-japonicum* by LC-MS/MS.

No	Compounds	RT (min)	exptl (m/z)	Characteristic fragment ions (m/z)
1	20-Hydroxyganoderic acid G	7.13	531.2936059	531.2934, 403.2093, 385.2003
2	Lucidenic acid N	7.29	483.2719262	483.3067, 465.2952, 447.2863
3	12-Deacetylganoderic acid H	7.61	553.2776707	553.2761, 535.2676, 277.0165
4	Ganoderic acid L	7.84	557.3083681	557.3101, 539.2947, 513.324
5	Lucidenic acid H	7.94	459.2751733	441.3008, 459.2785, 305.1368
6	(+)-Ganoderic acid K	8.05	575.3192949	575.3184, 461.2701, 479.2767
7	Methyl lucidete Q	8.08	457.293996	457.2934, 439.282, 173.0974
8	Ganoderenic acid B	8.08	497.2873471	497.2886, 439.2842, 343.1549
9	Lucidenic acid L	8.17	475.2696476	439.2527, 393.2431, 375.2681
10	Ganoderic acid O	8.65	529.2804997	381.2049, 365.2133, 475.2466
11	Ganolucidic acid C	8.65	541.3137196	541.3163, 523.3035, 465.2593
12	(+)-Lucidenic acid A	8.67	459.2752343	459.2743, 423.2533, 287.1258
13	(+)-Methyl lucidenic acid F	8.67	493.256873	493.258, 475.25, 447.2508
14	Lucidenic acid K	8.79	473.2543478	420.2261, 438.2377, 391.2248
15	Ganoderic acid G	8.90	515.2991448	515.2988, 367.2233, 479.2794
16	Ganoderic acid J	8.90	537.2823694	537.2786, 519.278, 5179.0667
17	Ganoderic acid M	8.93	553.277818	553.2761, 535.2676, 277.0165
18	Ganoderic acid F	9.20	571.2903362	377.2106, 571.2915, 363.1954
19	Ganoderenic acid D	9.27	513.2830255	513.28, 495.2806, 365.2068
20	Ganoderic acid H	9.27	595.2874748	595.2844, 535.2678, 291.1133
21	20(21)-Dehydrolycidenic acid A	9.68	457.2585917	421.2381, 457.2593, 381.207
22	Ganoderenic acid G	9.82	513.2847286	365.2111, 513.2852, 477.264
23	Ganoderiol D	10.53	489.3570003	471.3460, 453.3360, 413.3041
24	Ganoderic acid beta	10.76	523.3035401	523.3008, 505.2915, 419.2548
25	(+)-Ganolucidic acid D	10.78	483.3090452	483.3067, 465.2952, 447.2863
26	Ganolucidic acid E	11.60	467.3156741	467.3137, 337.2549, 449.3051
27	Echinocystic acid	11.79	473.3623119	473.3628, 455.3518, 259.1683
28	(-)-Ganoderic acid Ma	12.22	555.3651824	555.3609, 495.342, 215.1765
29	Lucidadiol	12.68	457.3672556	329.2473, 457.3665, 439.357
30	Ganodermanontriol	12.95	473.3523122	455.3517, 419.3323, 379.3016
31	Ganoderic acid Mk	12.98	553.3495507	553.3509, 495.3499, 105.0653
32	Ganoderic acid V	13.14	597.6293077	597.6293077, 581.564, 406.4467
33	Lucidone A	13.25	403.2464231	403.2445, 339.1919, 223.1299
34	(+)-Ganoderiol A	13.27	457.3677293	403.2445, 339.1919, 223.1299
35	Ganoderol B	13.91	437.3407329	437.3392, 145.1019, 213.1599
36	Ganoderiol B	13.91	471.346413	

**Table 2 (continued)**

No	Compounds	RT (min)	exptl (m/z)	Characteristic fragment ions (m/z)
37	(+)-Ganodermanondiol	14.65	439.3573715	471.3493, 269.1896, 453.3358
38	(+)-Methyl ganolucidate B	14.72	499.3422232	439.3561, 421.3467, 187.1475
39	Ganoderol A	15.20	437.3414754	499.3428, 481.345, 161.1376
40	Ganoderatriol	15.72	439.3570086	419.3314, 347.2566, 307.2641
41	Ganodermediol	15.76	423.362458	439.3571, 203.1806, 161.1334
42	Ganoderic acid X	16.01	495.3461849	423.3619, 159.1156, 145.1012
43	Ganoderic acid R	16.01	577.3508429	435.3257, 495.3446, 187.1492
44	Ganoderic acid S	16.22	453.3367435	577.3511, 517.325, 509.3255
45	Ganoderic acid DM	16.54	486.3582142	435.3249, 395.2939, 367.2631,
46	Ganoderic acid Y	16.63	437.3415454	315.2333, 149.1331, 486.3576
47	Ganoderol A	16.7	421.3466341	437.3401, 301.213, 161.1338
				421.3444, 159.1153, 171.1158

PYMOL and ligplus were used to carry out the quantification analysis of the stably binding of the compound to the binding site of the protein and interact with the surrounding amino acids. Using the CDOCKER docking module from PDB site records (NF- $\kappa$ B: 1IKN and Keap1: 1X2R), the docking results will show the binding pattern between the different conformations of the small molecule ligand and the protein.

## 2.8. Data analysis

All experiments were performed in three independent replicates. Statistical analysis was performed using GraphPad Prism software and SPASS software, and the data were presented as mean  $\pm$  SD. Correlations and *p*-values of experimental results were assessed by one-way analysis of variance (ANOVA) calculations and Student's T-test. *p* < 0.05 was considered significant.

## 3. Results and discussion

### 3.1. Characterization and biological activities of the crude extracts and fractions

#### 3.1.1. Total triterpene content of the crude extracts

Research on biologically active fractions has shown that *Ganoderma* triterpenoids have multiple functions, which has led to extensive study of their enclosed features, including antitumor, antioxidant, and sedative properties. Therefore, the total triterpene content of the crude extract was determined in this study. The concentration of the standard product and the absorbance of the corresponding solution were fitted to the standard curve for the determination of the total triterpene content (Fig. S2). The regression coefficient  $R^2$  was greater than 0.9992, indicating good linear relationship within the selected concentration range. The total triterpene content in the crude extracts of *G. neo-japonicum* was 83.4 mg/g according to the standard curve.

#### 3.1.2. Component identification of crude extracts using UHPLC-Triple TOF-MS/MS

The total ion current (TIC) chromatogram of the extracts is shown in Fig. S3. The exact mass-to-charge ratio (*m/z*) of the compound was obtained by TOF-MS, while the second-order fragment ion of this mass

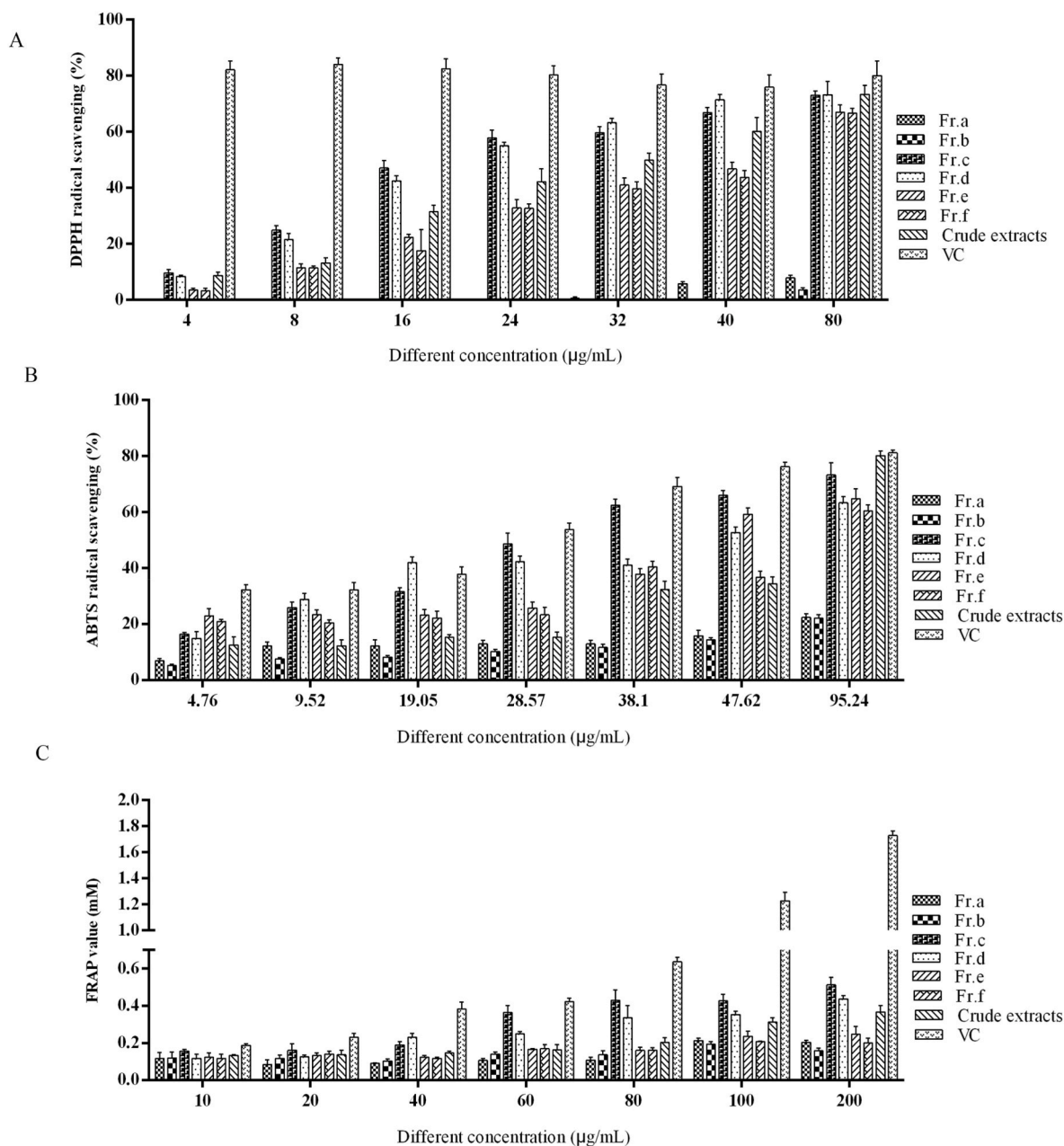


Fig. 1. Effects of the different fractions, crude extract and control group vitamin C (Vc) to scavenge DPPH radical (A), ABTS radical (B), and FRAP radical (C).

number was obtained by product ion secondary. The triterpenoids of the crude extracts were identified by analyzing the corresponding cracking law matching method for the peaks containing  $\text{MS}^2$  ion fragments. A total of 47 triterpenoids in the crude extracts were identified based on accurate comparisons between experimental ions ( $[\text{M}-\text{H}]^+$ ) on positive mode, calculated ions, and characteristic fragment ions obtained from the in-house  $\text{MS}^2$  database (Table 2), which was created based on the mass spectrometric data of more than two thousand Chinese herbal medicine compounds.

### 3.1.3. Antioxidant ability analysis of all fractions

Previous studies have demonstrated that triterpenes and polysaccharide compounds extracted from *G. lucidum* have significant antioxidant effects (Pan et al., 2022; Shizhong Zheng et al., 2020). *In vitro* and *in vivo* experiments showed that the total triterpenes isolated from *G. lucidum* in South India had strong free radical scavenging ability and enhanced the body's defense function (Smina, Mathew, et al., 2011).

Therefore, we guessed whether the multiple components isolated from *G. neo-japonicum* had antioxidant activity. In this study, different antioxidant assays (DPPH, ABTS, and FRAP) were performed for the six fractions Fr. (a), (b), (c), (d), (e), (f) and the crude extract.

In the DPPH assay, the radical scavenging rates of all the samples increased according to concentration augmented (Fig. 1A and Table S1). From Table S1, the DPPH free radical scavenging ability of Fr (c) was the strongest ( $\text{EC}_{50} = 22.108 \mu\text{g/mL}$ ) compared with other fraction and the crude extract.

The ABTS and FRAP results are displayed in Fig. 1B–C, respectively. The  $\text{EC}_{50}$  value of the ABTS and FRAP are shown in Table S1. According to the previous results, the ABTS  $\text{EC}_{50}$  value of Fr (c) was the lowest ( $26.331 \mu\text{g/mL}$ ). In addition, the results in Fig. 1B indicated that the Fr (c) has the highest scavenging rate at concentrations between 26 and 95  $\mu\text{g/mL}$ . Similarly, in the FRAP experiment, Fr (c) also showed a relatively stronger effect than that of other samples at concentrations of 60–200  $\mu\text{g/mL}$ . In general, this indicates that the test sample has strong

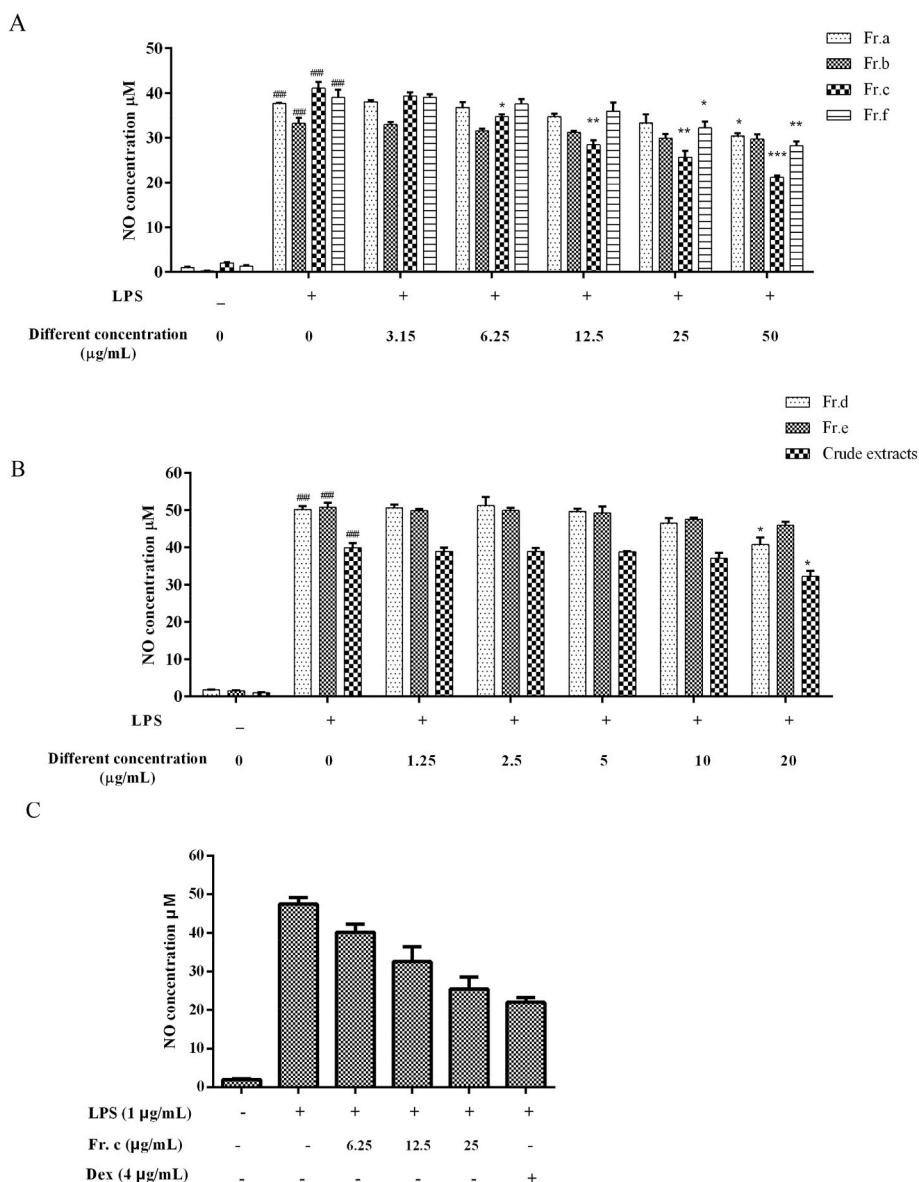


Fig. 2. Effects of all fractions (Fr. (a)–(f) and crude extracts) on RAW264.7 cells viability. Data are expressed as the mean ± SD (n = 3). \*\*\*p < 0.001, \*\*p < 0.01, \*p < 0.05 as compared to the control.

antioxidant activity, so *G. lucidum* may be a new resource for exploring natural antioxidants.

### 3.1.4. Potential anti-inflammatory effect of all fractions

Oxidative stress levels determine the immune response of the body and regulate the production of inflammatory cytokines during viral infection (Dragomanova et al., 2021). Although inflammation is a protective immune function against pathogen infection and danger signals, excessive and continuous inflammation can cause tissue damage and functional obstacles (Z. Liu et al., 2018; Peng et al., 2020). Anti-inflammatory therapy is also one of the effective strategies to suppress the cytokine storm of COVID-19 infection and other inflammatory diseases. It has been reported that *G. lucidum* potential antiviral and immunomodulatory properties combinedly exhibit remarkable importance in present pandemic COVID-19 (Hetland et al., 2021).

Based on the reported species of *G. lucidum*, it has excellent anti-inflammatory activity, and immune regulating activities (Dudhgaonkar et al., 2009; Shao et al., 2021). Next, a preliminary evaluation of the potential anti-inflammatory effect of all ingredients (Fr. (a)–(f) and crude extracts) samples from *G. neo-japonicum* was performed.

**3.1.4.1. Effect on RAW264.7 cell viability.** The potential cytotoxicity of all fractions (Fr. (a)–(f) and crude extracts) and their effects on the viability of RAW264.7 cells were tested by CCK-8 assay. As shown in Fig. 2A–G, Fr. (a) and (b) had no effect on the viability of RAW264.7 cells at a concentration lower than 100 µg/mL. Fr. (c) and (f) had no effect on cell growth when they are lower than 60 µg/mL. However, Fr. (d) and (e) showed cytotoxicity to RAW 264.7 cells at a concentration of 20 µg/mL, and cell viability was significantly reduced at 40 µg/mL. The same behavior was observed for the crude extract. Therefore, we chose a concentration range that is safe for cell viability for follow-up inflammation studies.

**3.1.4.2. Effect on LPS-mediated production of NO in RAW264 cells.** To evaluate the anti-inflammatory activity of all fractions (Fr. (a)–(f) and crude extracts), the level of NO was detected in RAW264.7 cells after LPS stimulation. Excessive production of NO can destroy the normal tissue cells of the body and is involved in the occurrence and development of many diseases, especially in the occurrence of inflammation and signal transduction (Xue et al., 2018). As shown in Fig. 3A–C, LPS (1

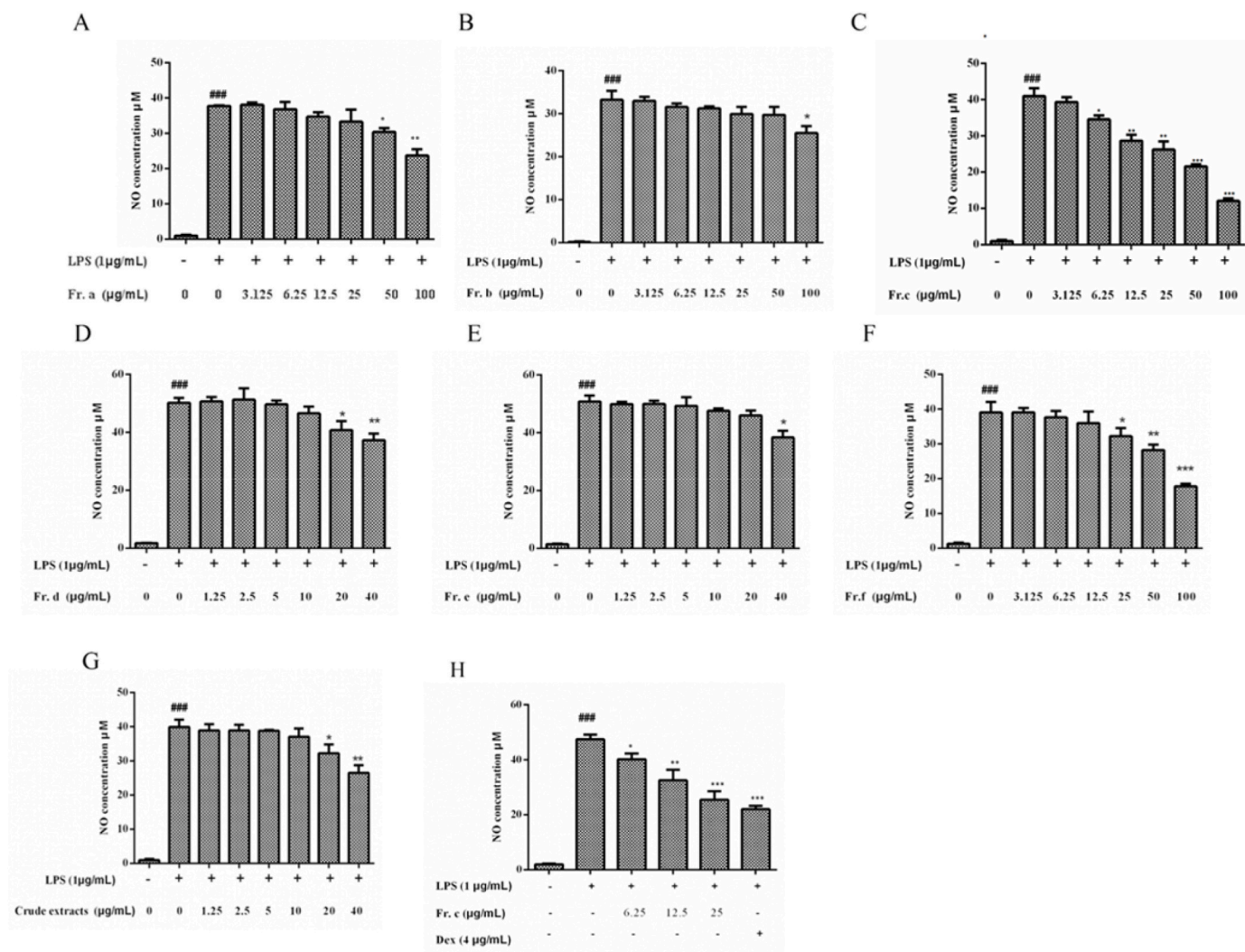


**Fig. 3.** Effect of all fractions (Fr. (a)–(f) and crude extracts) on LPS-mediated production of NO in RAW264 cells. Cells were pre-treated with various concentrations of *Ganoderma* fractions or Dex (positive control, 4 µg/mL) for 2 h and were co-treated with LPS (1 µg/mL) for 18 h. NO levels in the cell culture media were determined using a Griess assay. Data shown are expressed as the mean ± SD (n = 3). ###p < 0.001 when compared with control versus LPS; \*\*\*p < 0.001, \*\*p < 0.01, \*p < 0.05 as compared to the group treated with LPS alone.

µg/mL) stimulation significantly upregulated the release of NO to 30–40 times the level of the control. By comparing all tested samples with the positive control dexamethasone 4 µg/mL (10 µM), it can be found that Fr. (c) was significantly effective in inhibiting NO production in LPS-induced RAW264.7 cells when the concentration was lower than 25 µg/mL, whereas no significant cell death was observed at this concentration. Ganoluciduone A, a new lanostanoid compound isolated from *Ganolucidum* for the first time, inhibits NO production in LPS-activated RAW264.7 cells and exerts anti-inflammatory activity (Su et al., 2020). In addition, Ganoderic Acid A inhibited IL-1β -induced NO in nucleus

pulposus cells and may have anti-inflammatory effects on intervertebral disc degeneration inflammation (Sihua Zheng et al., 2022). Therefore, we believe that the Fr. (c) component may have potential anti-inflammatory activity in LPS-induced RAW264.7 cells. Next, we selected Fr. (c) concentrations of 6.25, 12.5, and µg/mL for further investigation.

**Table 3**  
The identification results of the triterpenoids in Fr. (c) by LC-MS/MS.

No	Compounds	RT (min)	exptl (m/z)	calcd (m/z)	Fragment ions (m/z)
1	Lucidenic acid L	9.873	475.2696476	474.59	439.2494, 411.2538, 403.2279, 393.2433, 375.2328, 361.2163, 357.2227
2	Ganoderiol D	11.656	489.3570003	488.71	471.3460, 453.3360, 413.3041, 395.2922
3	Ganoderic acid beta	12.103	523.3035401	522.6	511.3390, 505.2915, 419.2548, 471.3469, 465.2987, 453.3360, 435.3250
4	Ganoderic acid F	43.981	571.2903362	570.67	511.2695, 493.2596, 475.2475, 457.2387, 429.2408, 377.2106
5	Ganoderenic acid B	44.984	497.2873471	516.7	457.2952, 439.2842, 365.1362, 343.1549
6	Ganodermanontriol	54.535	473.3523112	472.7	455.3531, 437.3426, 419.3323, 379.3016
7	Ganoderic acid S	55.174	453.3367435	452.67	435.3249, 395.2939, 341.2472, 367.2631, 325.2525,
8	Ganoderal A	59.087	437.3414754	436.66	419.3314, 347.2566, 325.1811, 307.2641

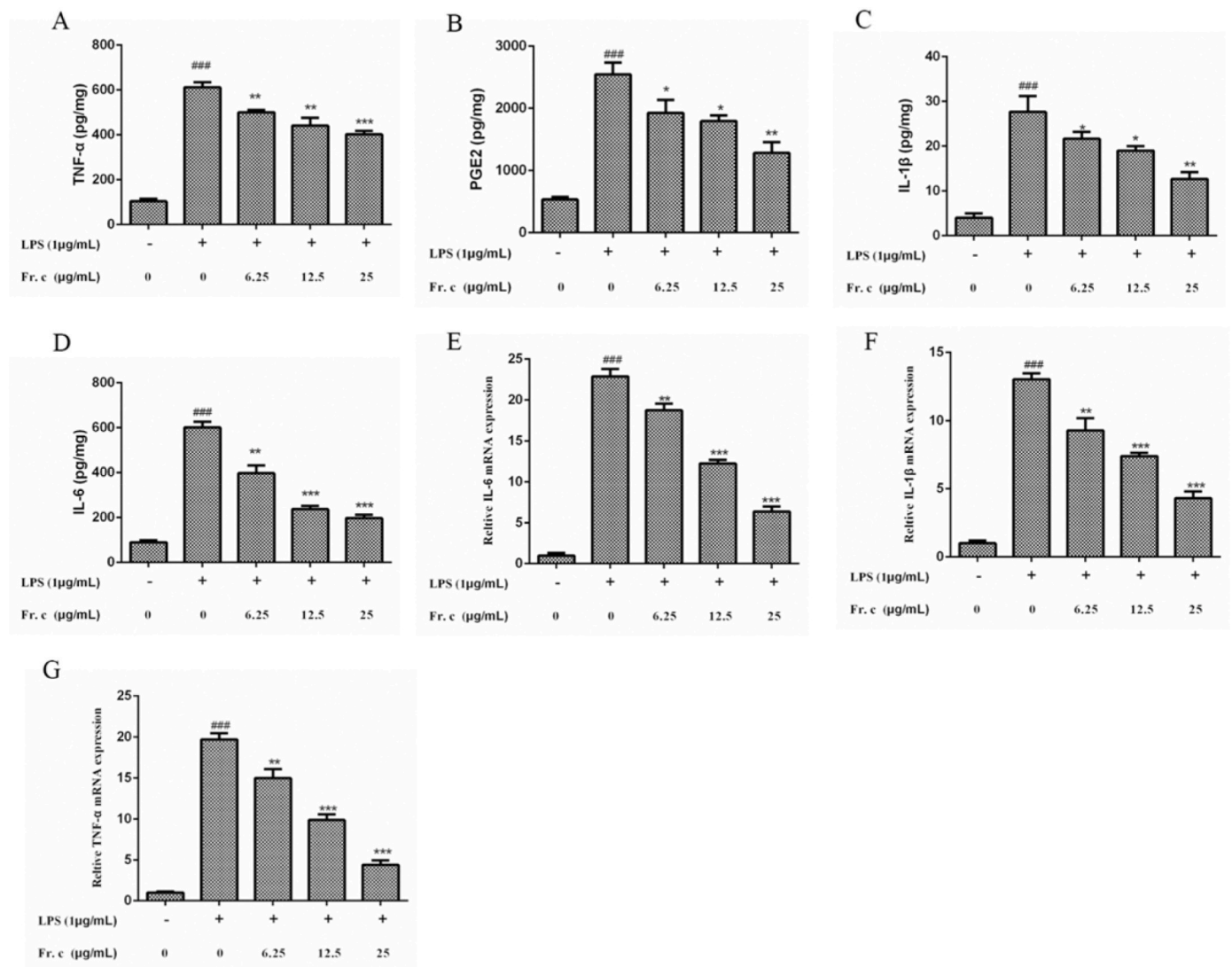


**Fig. 4.** Effects of Fr. (c) on the production of LPS-induced pro-inflammatory cytokines in RAW264.7 cells. The expression level of TNF- $\alpha$  (A), PGE2 (B), IL-1 $\beta$  (C) and IL-6 (D) were measured as described in the materials and method. The mRNA expression level of IL-6 (E), IL-1 $\beta$  (F), TNF- $\alpha$  (G) were measured by RT-qPCR in the RAW264.7 cells. Data shown represent the mean  $\pm$  SD (n = 3). ### $p$  < 0.001 when compared with control versus LPS; \*\*\* $p$  < 0.001, \*\* $p$  < 0.01, \* $p$  < 0.05 as compared to the group treated with LPS alone.

### 3.2. Characterization and biological activities of Fr. (c)

#### 3.2.1. Component identification of Fr. (c) using UHPLC-triple TOF-MS/MS

Based on the previous tests, the Fr. (c) had the best antioxidant and anti-inflammatory effects compared with the other fractions. The total triterpene content of the Fr. (c) was 483.15 mg/g calculated according to the method of section 2.4. The triterpene composition of Fr. (c) was identified by LC-MS/MS and a total of 8 triterpenoids were determined as Lucidenic acid L, Ganoderiol D, Ganoderic acid beta, Ganoderic acid F, Ganoderenic acid B, Ganodermanontriol, Ganoderal A, and Ganoderic acid S, through database and purchased standard substances. The MS data of all confirmed compounds, including the observed ion mass, theoretical ion mass, parent ions, main fragments in the positive ion mode, and the proposed compounds, are exhibited in Table 3 and Fig. S4. In addition, the structural formulas and HPLC chromatograms of eight triterpenoids are shown in Fig. 8, respectively.

#### 3.2.2. Potential anti-inflammatory effect of fraction Fr. (c)

##### 3.2.2.1. Effects on production of LPS-induced proinflammatory cytokines in RAW264.7 cells. Activated macrophages can produce a variety of

different inflammatory mediators such as TNF- $\alpha$ , IL-1 $\beta$ , IL-6 and PGE2, which participate in a variety of inflammatory processes and induce various inflammatory related diseases (Jaiswal et al., 2000). Therefore, inhibiting the release of these inflammatory factors is a key target for the treatment of inflammatory related diseases. To study the effects of Fr. (c) in the production of pro-inflammatory factors in LPS-induced RAW264.7 cells, the expression level of each molecule in the RAW264.7 culture supernatant was determined by ELISA experiments. As shown in Fig. 4A–D, the overproduction of IL-1 $\beta$ , IL-6, TNF- $\alpha$ , and PGE2 induced by LPS was significantly inhibited after the treatment with Fr. (c), and the expression level decreased in a concentration-dependent manner. Secretion of TNF- $\alpha$ , IL-1 $\beta$  and IL-6 proteins should be closely related to their gene expressions. Similar results were obtained in the detection of mRNA levels of proinflammatory factors for TNF- $\alpha$ , IL-1 $\beta$  and IL-6 (Fig. 4E–G), suggesting that Fr. (c) may suppress inflammation production by regulating gene transcription levels of pro-inflammatory factors.

##### 3.2.2.2. Effect on iNOS and COX-2 expression in LPS-mediated RAW264.7 cells.

In one hand, since NO is synthesized by nitric oxide synthase (iNOS), the release of NO is closely related to the expression of

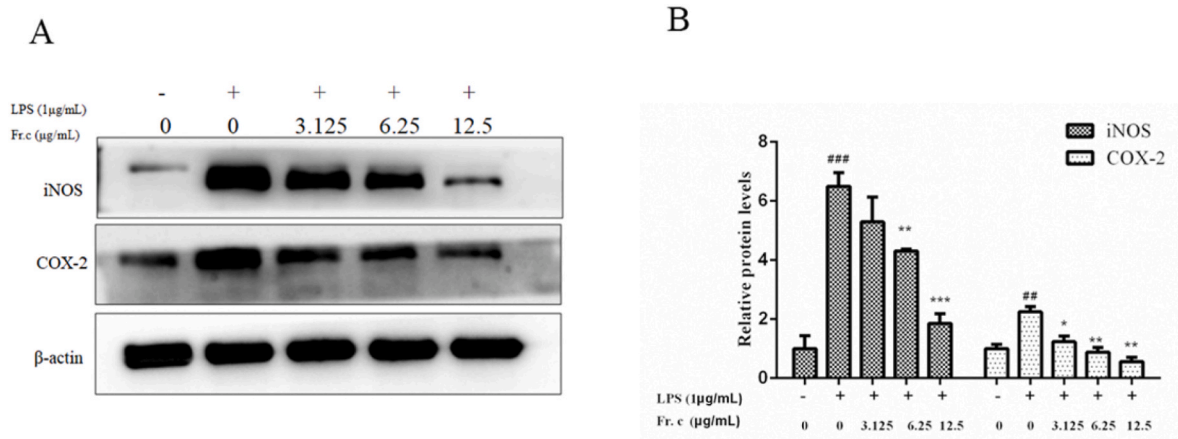


**Fig. 5.** Effects of Fr. (c) on iNOS and COX-2 protein expressions in LPS-stimulated RAW264.7 cells. RAW264.7 macrophages were pretreated with various concentrations Fr. (c) for 2 h, then was co-treated with LPS (1 µg/mL) for 18 h. The expression levels of iNOS and COX-2 were detected using Western blot analysis. Data shown represent the mean ± SD (n = 3). ###p < 0.001 when compared with control versus LPS; \*\*\*p < 0.001, \*\*p < 0.01, \*p < 0.05 as compared to the group treated with LPS alone.

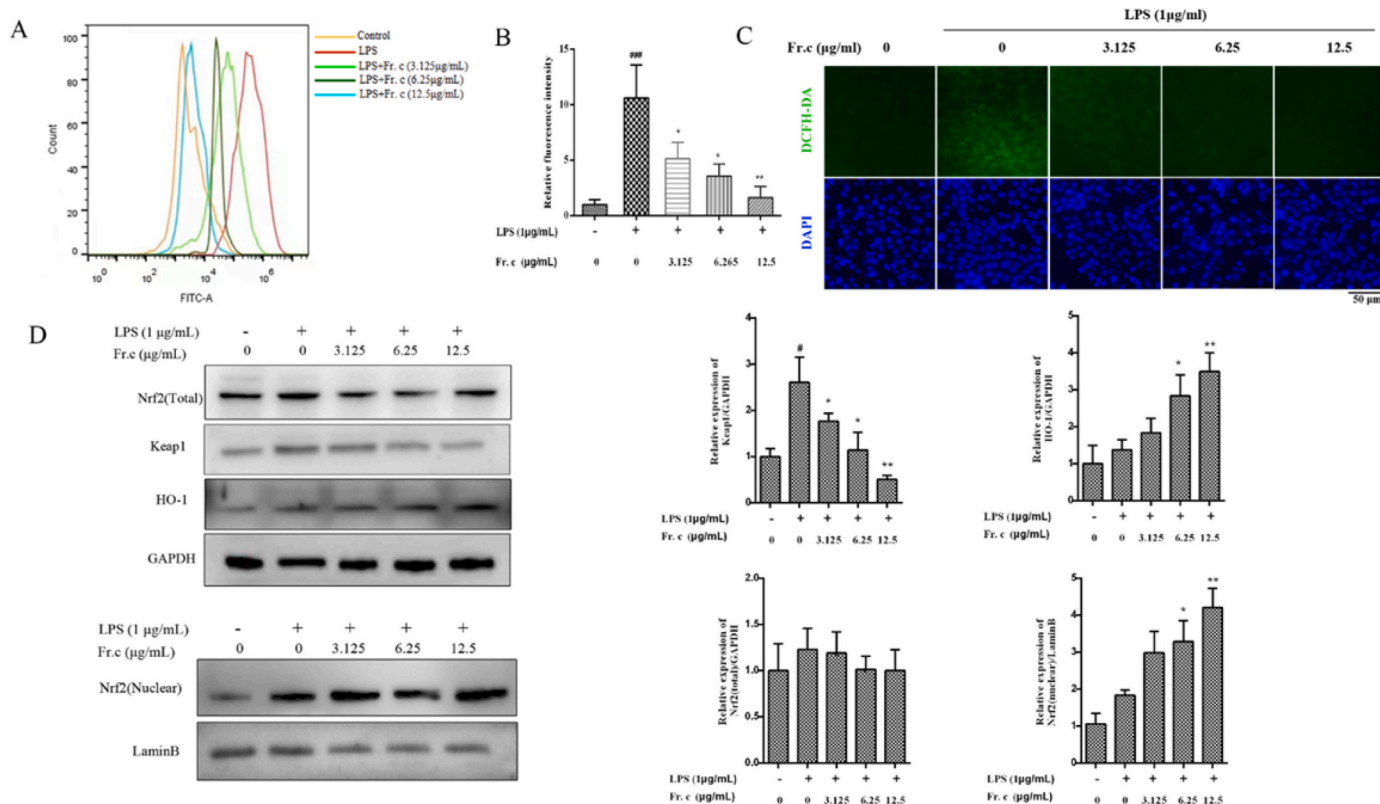


**Fig. 6.** Effects of Fr. (c) on LPS-mediated oxidative stress in RAW264.7 cells. RAW264.7 cells were pretreated with various concentrations of Fr. (c) for 2 h, then was co-treated with LPS (1 µg/mL) for 18 h. After loading the DCFH-DA fluorescent probe, intracellular ROS were detected using flow cytometry and fluorescence microscopy. Nuclei is stained with DAPI, whereas DCFH is shown as green fluorescence (A–C). The expression levels of Nrf2, HO-1 and Keap1 were detected using Western blot analysis (D). Data shown represent the mean ± SD (n = 3). ###p < 0.001 when compared with control versus LPS; \*\*\*p < 0.001, \*\*p < 0.01, \*p < 0.05 as compared to the group treated with LPS alone. (For interpretation of the references to color in this figure legend, the reader is referred to the Web version of this article.)

iNOS. In the other hand, COX-2, as an important pro-inflammatory protein, is involved in the expression of various inflammatory factors (Kim and Kim, 2017; Lee et al., 2017). Therefore, reducing the expression of iNOS and COX-2 reduces the release of proinflammatory factors, thus producing anti-inflammatory effects. This study further evaluated COX-2 and iNOS expression after Fr. (c) treatment. As shown in Fig. 5, the expression levels of iNOS and COX-2 in RAW264.7 cells increased

significantly after LPS stimulation, which is consistent with the expression of pro-inflammatory factors observed above. However, in the groups treated with the Fr. (c), the expression of COX-2 and iNOS had a dose-dependent inhibitory effect. These studies showed that Fr. (c) may have an anti-inflammatory effect by downregulating the expression of iNOS and COX-2.

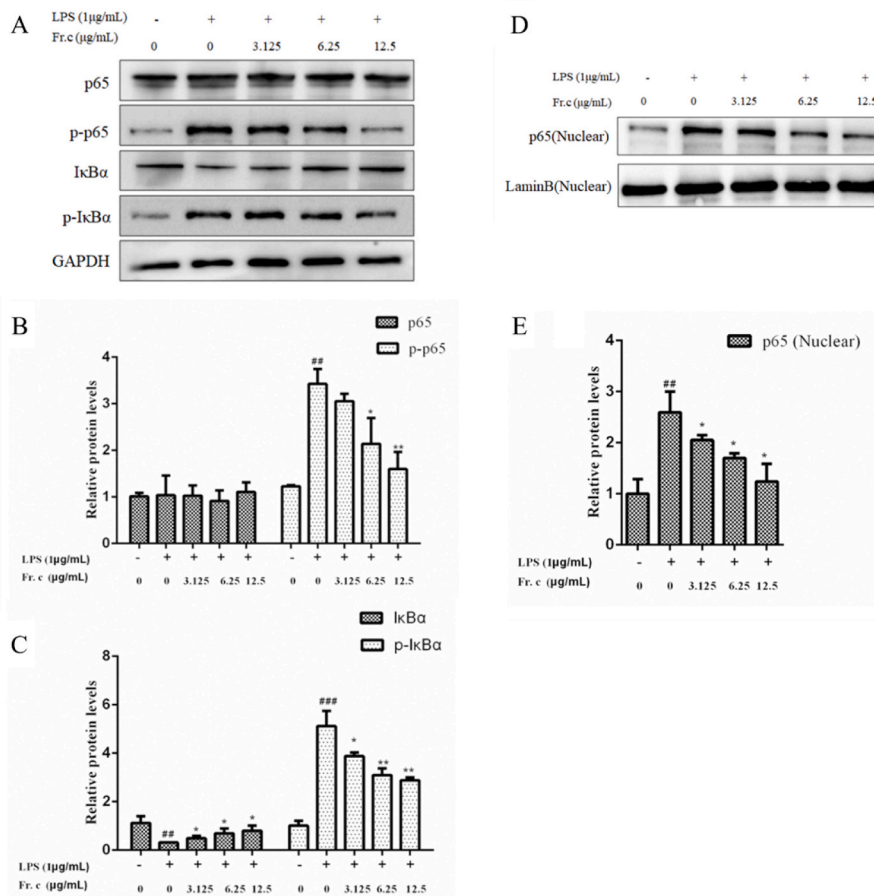


**Fig. 7.** Effects of Fr. (c) on NF- $\kappa$ B protein expression in LPS-stimulated RAW264.7 cells. RAW264.7 macrophages were pretreated with various concentrations of Fr. (c) for 2 h, then was co-treated with LPS (1  $\mu$ g/mL) for 18 h. The expression levels of I $\kappa$ B $\alpha$ , p-I $\kappa$ B $\alpha$ , P65, and p-P65 in the nucleus were detected using Western blot analysis. Data shown represent the mean  $\pm$  SD (n = 3). ### $p$  < 0.001 when compared with control versus LPS; \*\*\* $p$  < 0.001, \*\* $p$  < 0.01, \* $p$  < 0.05 as compared to the group treated with LPS alone.

**3.2.2.3. Effects on oxidative stress in LPS-mediated RAW264.7 cells.** It has been reported that activation of inflammasome can trigger mitochondrial damage and ROS production (Platnich et al., 2018), and when ROS is overproduced *in vivo*, it induces cellular oxidative damage and is an important indicator of oxidative stress [37]. In turn, reducing the level of ROS in mitochondria or inhibiting redox pathways can alleviate the occurrence of inflammation (Park et al., 2015). In the above experiments, we detected that Fr. (c) had strong antioxidant activity and inhibits LPS induced release of inflammatory factors. Some studies have shown that *G. lucidum* triterpenoid extract increases the activity of superoxide dismutase and catalase enzymes, enzymes involved in scavenging ROS, reducing and eliminating oxidative damage (Smina, De, et al., 2011). Therefore, it was hypothesized that Fr. (c) may play a role in LPS-mediated oxidative stress. The levels of ROS in RAW264.7 cells in different treatment groups were detected by DCFH-DA fluorescent probe. As shown in Fig. 6A–C, green fluorescence was significantly increased in RAW264.7 cells after LPS treatment. However, after Fr. (c) treatment, the fluorescence intensity gradually weakened and the level of ROS was significantly reduced, which was verified by fluorescence microscopy and flow cytometry. These results showed that Fr. (c) could inhibit the production and accumulation of ROS induced by LPS in RAW264.7 cells.

To determine the mechanism by which Fr. (c) inhibits LPS-induced oxidative stress, we examined the expression of Kelch-like ECH-associated protein 1 (Keap1), Nrf2 and the downstream heme oxygenase-1 (HO-1). Nrf2 is one of the major regulators of cellular defense against oxidative stress, with antioxidant and anti-inflammatory properties (D. D. Zhang and Chapman, 2020). Under normal physiological conditions, Nrf2 is localized in the cytoplasm and binds to Keap1, which is then degraded through the ubiquitin proteasome pathway. Under oxidative

stress, Nrf2 is released from Keap1 and transferred to the nucleus. As a nuclear transcription factor, Nrf2 initiates the expression of a series of downstream antioxidant enzymes including HO-1 (Loboda et al., 2016; Yamamoto et al., 2018). As shown in Fig. 6D, in RAW264.7 cells after LPS stimulation, the results showed that Fr. (c) effectively increased the expression of Nrf2 in the nucleus and HO-1 protein, while reducing the expression of its negative regulator Keap1. Studies have shown that HO-1 blocks LPS-induced inflammation by inhibiting the release of various pro-inflammatory factors (Choi et al., 2014). In this study, Fr. (c) treatment effectively inhibited the release of inflammatory mediators, which may be somewhat dependent on the expression of HO-1. At the same time, we believe that there is also a correlation between an increase in HO-1 levels and a decrease in ROS. Overall, our results suggest that Fr. (c) can exert an anti-inflammatory effect by inhibiting oxidative damage.

**3.2.2.4. Effects on regulating NF- $\kappa$ B activation in LPS-mediated RAW264.7 cells.** Activation of Nrf2/HO-1 signaling pathway may inhibit LPS-induced NF- $\kappa$ B activation and production of various inflammatory cytokines including NO (Wang et al., 2018). Next, we examined the effect of Fr. (c) on the activation of the NF- $\kappa$ B signaling pathway. NF- $\kappa$ B ( p65 ) is a nuclear transcription factor that regulates inflammatory responses by controlling the release of pro-inflammatory factors and gene expression (Tak and Firestein, 2001). Under normal conditions, I $\kappa$ B $\alpha$  and NF- $\kappa$ B form a complex that stably exists in the cytoplasm. When cells are stimulated by LPS, I $\kappa$ B $\alpha$  is phosphorylated and degraded, and unbound p65 is detached from I $\kappa$ B $\alpha$  and subsequently translocated to the nucleus, thereby activating the transcription of its target genes and the expression of pro-inflammatory factors (Natoli and Chiocca, 2008; Tak and Firestein, 2001; Xu et al., 2021). As shown in

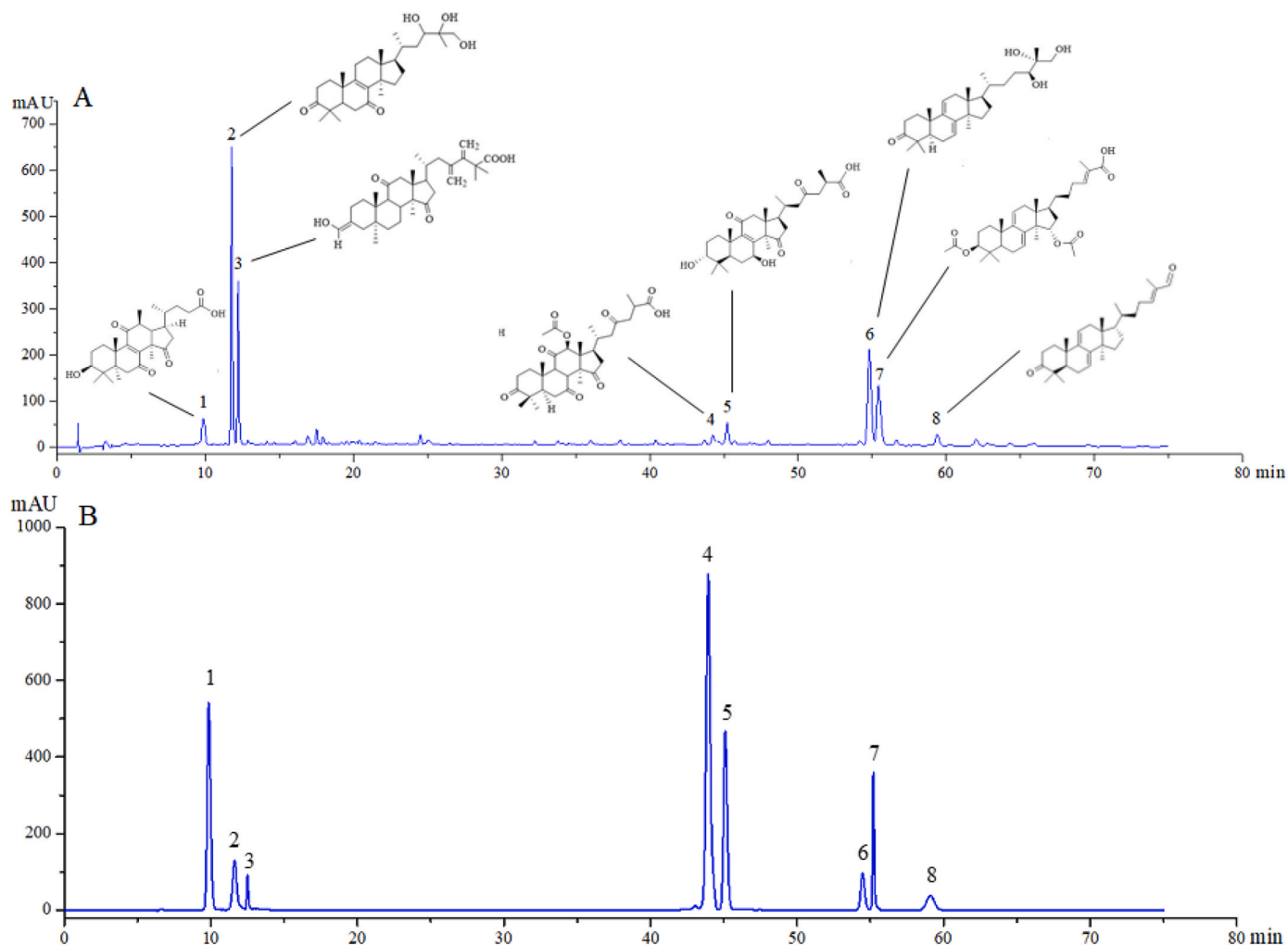


**Fig. 8.** HPLC chromatograms of triterpenoids from (A) Fr. (c) and (B) standard substance; Lucidenic acid L (1), Ganoderiol D (2), Ganoderic acid beta (3), Ganoderic acid F (4), Ganoderenic acid B (5), Ganodermanontriol (6), Ganoderic acid S (7), and Ganoderal A (8).

**Table 4**  
Target protein docking results for compounds.

Compound	NF- $\kappa$ B (Binding Energy, kcal/mol)	Keap1 (Binding Energy, kcal/mol)
Ganoderiol D	-8.1	-10.0
Ganoderic acid beta	-8.3	-9.8
Ganodermanontriol	-7.9	-11
Ganoderic acid S	-7.9	-9.4
Ganoderenic acid B	-8.5	-8.6
Ganoderal A	-7.9	-7.9
Ganoderic acid F	-8.0	-8.6
Lucidenic acid L	-9.9	-7.9

Fig. 7A–C, when LPS alone acted on RAW264.7 cells, the expression of p-P65 and p-I $\kappa$ B $\alpha$  was significantly increased by 3 times compared with that of the control group. In contrast, treatment with 6.25–12.5  $\mu$ g/L Fr. (c) reduced the LPS-induced phosphorylation of I $\kappa$ B $\alpha$  and p65 in a dose-dependent manner. In this study, we found that Fr. (c) significantly inhibited LPS-induced degradation of I $\kappa$ B $\alpha$  and the p65 translocation from cytosol to nucleus (Fig. 7D–E). These data suggest that the potential anti-inflammatory mechanism of Fr. (c) is related to the suppression of NF- $\kappa$ B activation in macrophage RAW264.7 cells.

### 3.2.3. Molecular docking

The strong antioxidant and anti-inflammatory activity of Fr. (c) may

be attributed to the triterpenoid type contained in it. Next, we conducted molecular docking studies on the majority components in Fr. (c) (including Ganoderiol D, Ganoderic acid beta, Ganodermanontriol and Ganoderic acid S) with nuclear transcription factors NF- $\kappa$ B and Keap1 to explore their binding modes. It is noteworthy that the four *G. neo-japonicum* triterpenes showed low binding energy values (i.e., higher affinities) to both target proteins, as shown in Table 4. The binding energies of the four triterpenes (Ganoderiol D, Ganoderic acid beta, Ganodermanontriol and Ganoderic acid S) to Keap1 ranged from -11 to -9.4 kcal/mol, and the binding energies of NF- $\kappa$ B ranged from -7.9 to -8.1 kcal/mol, indicating that the binding affinities of the four triterpenes to the two target proteins were similar. In addition, we also tested the binding activity of the remaining four triterpenes (Lucidenic acid L, Ganoderal A, Ganoderic acid F, Ganoderenic acid B) to NF- $\kappa$ B and Keap1, although their content in Fr. (c) component was low. The binding energies to Keap1 ranged from -7.9 to -8.6 kcal/mol, and the binding energies of NF- $\kappa$ B ranged from -7.9 to -9.0 kcal/mol, as shown in Table 4 and Fig. S5.

The docking results showed a strong binding between four *G. neo-japonicum* triterpenes and Keap1, which formed several hydrogen bonds with nearby amino acid residues, including VAL-463, VAL-465 and ARG-326 in Ganoderiol D, and VAL-420 in Ganoderic acid beta, ALA-510, THR-560, VAL-561, LEU-557 in Ganodermanontriol, and VAL-465, VAL-512, VAL-514 in Ganoderic acid S. Besides hydrogen bonds, many Van der Waals, carbon hydrogen bond and pi-alkyl interactions

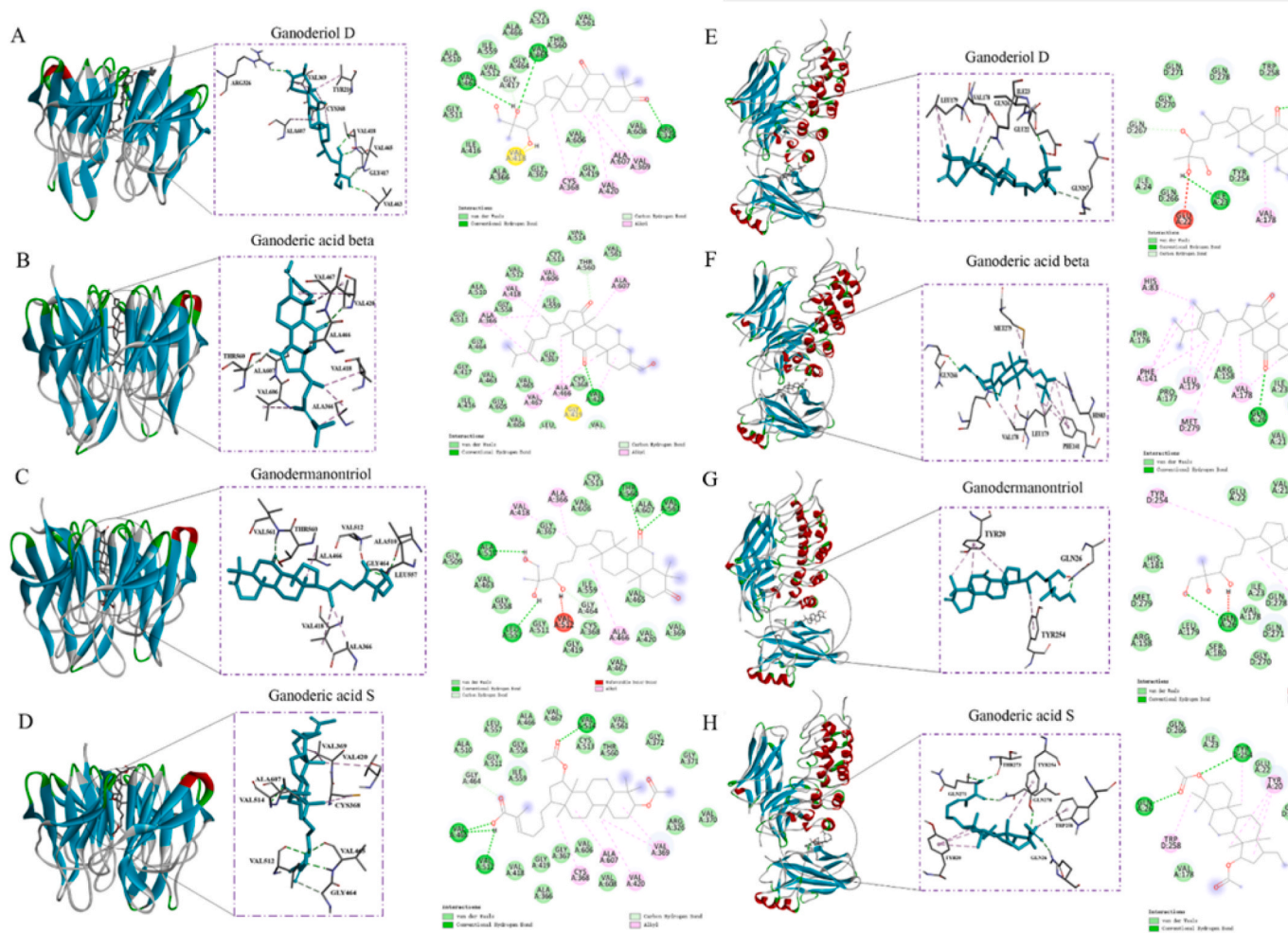


Fig. 9. Visualization for molecular docking between the 4 *G. neo-japonicum* triterpenes and (A–D) Keap1 (PDB:1X2R) and (E–H) NF- $\kappa$ B (PDB:1IKN).

were also showed in Fig. 9A–D. The four compounds bind to the same domain but have different amino acids in this pharmacophore. Like Keap1, the four compounds were bound to the same domain of NF- $\kappa$ B, which formed several hydrogen bonds with nearby amino acid residues, including ILE-23 and GLN-26 in Ganoderiol D, and GLN-26 and GLN-266 in Ganoderic acid beta, and GLN-26 in Ganodermanontriol, and GLN-26, GLN278, THR-273, and GLN-271 in Ganoderic acid S, as shown in Fig. 9E–F. Ganodermanontriol showed strong binding to Keap1 protein, which may be attributed to the combination of more hydrogen bonds. At the same time, it has been reported that Ganodermanontriol plays an anti-inflammatory role by activating the nuclear translocation of NRF protein and inhibited the expressions of TLR4 and MyD88 *in vivo*, while protecting hepatic cell from t-BHP mediated oxidative stimulus (Ha et al., 2013; Hu et al., 2020). A recent report shows that Ganoderiol D targets 14-3-3 $\epsilon$  Activating CaM/CaMKII/NRF2 signaling pathway to enhance antioxidant capacity and delay aging in mesenchymal stem cells (Yuan et al., 2022). Ganoderic acid F plays a role in neural inflammation associated diseases by regulating NF- $\kappa$ B pathway (Sheng et al., 2020). These studies further support the anti-inflammatory and antioxidant activities of Fr. (c) components. Although our results show that Lucidenic acid L, Ganoderic acid beta, Ganoderic acid S and Ganoderic acid B have a certain binding energy to NF- $\kappa$ B and Keap1, which may also be an important target for them to play a role, their anti-inflammatory and antioxidant activities have not yet been reported. However, our molecular docking results may be an important basis for studying their potential biological activities.

#### 4. Conclusion

In conclusion, *G. neo-japonicum* is rich in a variety of terpenoids, and 47 triterpenoids were identified by UHPLC-Triple TOF-MS/MS. Then, the crude extracts were subjected to column chromatography to obtain six fractions Fr. (a), (b), (c), (d), (e) and (f), among which Fr. (c) was found to exhibit the strongest bioactivity for antioxidant and anti-inflammatory effects. Eight triterpenoids, namely Lucidenic acid L, Ganoderiol D, Ganoderic acid beta, Ganoderic acid F, Ganoderic acid B, Ganodermanontriol, Ganoderic acid S, and Ganoderic acid A in Fr. (c) were identified in combination by LC-MS/MS. In conclusion, the current study shows that Fr. (c) reduces LPS-induced inflammation and oxidative stress by inhibiting the activation of the NF- $\kappa$ B pathway and activating the NRF2/HO-1 pathway. This paper could provide a scientific theoretical basis for the further utilization of *G. neo-japonicum*.

After *G. lucidum* was approved as general food in some areas of China (State Health Office Food Letter No. 2018278), such as Shandong Province, *Ganoderma* industry expects a great development. Therefore, this research about the antioxidant and anti-inflammatory ability of the active fractions in *G. neo-japonicum* provides the basis for further development and utilization of this mushroom. In the future, Fr. (c) of *G. neo-japonicum* is expected to become a functional food for health and longevity because its composition and activity mechanism.

## Ethical statement

This research did not include any human subjects and animal experiments.

## CRedit authorship contribution statement

**Rui-rui Zhang:** Conceptualization, Methodology, Validation, Investigation, Writing – original draft. **Jing Zhang:** Conceptualization, Methodology, Validation, Investigation, Writing – original draft. **Xu Guo:** Conceptualization, Data curation, Formal analysis. **Ying-ying Chen:** Conceptualization, Formal analysis. **Jin-yue Sun:** Conceptualization, Formal analysis. **Jia-lin Miao:** Conceptualization, Formal analysis. **M. Carpena:** Conceptualization, Formal analysis. **M.A. Prieto:** Resources, Methodology, Funding acquisition, Writing – review & editing, Supervision. **Ning-yang Li:** Resources, Methodology, Funding acquisition, Writing – review & editing, Supervision. **Qing-xin Zhou:** Resources, Methodology, Writing – review & editing, Supervision. **Chao Liu:** Resources, Methodology, Writing – review & editing, Supervision.

## Declaration of competing interest

The authors declare that they have no known competing financial interests or personal relationships that could have appeared to influence the work reported in this paper.

## Data availability

No data was used for the research described in the article.

## Acknowledgements

This study was supported by the Provincial Key Research and Development (Major Scientific and Technological Innovation) Program of Shandong, China (NO. 2021SFGC0904; 2021TZXD001; 2021TZXD004); the Natural Science Foundation of Shandong, China (No. ZR2020MH401, ZR2021QH351); the National Key R&D Program of China (NO. 2021YFE0109200); the Taishan Scholars's Program of Shandong for Jinyue-Sun. The research leading to these results was supported by MICINN supporting the Ramón y Cajal grant for M.A. Prieto (RYC-2017-22891); by Xunta de Galicia for supporting the program EXCELENCIA-ED431F 2020/12 and the pre-doctoral grant of M. Carpena (ED481A 2021/313).

## Appendix A. Supplementary data

Supplementary data to this article can be found online at <https://doi.org/10.1016/j.crfs.2023.100441>.

## References

- Ajith, T.A., Sudheesh, N.P., Roshny, D., Abishek, G., Janardhanan, K.K., 2009. Effect of Ganoderma lucidum on the activities of mitochondrial dehydrogenases and complex I and II of electron transport chain in the brain of aged rats. *Exp. Gerontol.* 44 (3) <https://doi.org/10.1016/j.exger.2008.11.002>.
- Cao, Y., Wu, S.H., Dai, Y.C., 2012. Species clarification of the prize medicinal Ganoderma mushroom Lingzhi. *Fungal Divers.* 56 (1) <https://doi.org/10.1007/s13225-012-0178-5>.
- Chen, H., Zhang, J., Ren, J., Wang, W., Xiong, W., Zhang, Y., Bao, L., Liu, H., 2018. Triterpenes and meroterpenes with neuroprotective effects from ganoderma leucocontextum. *Chem. Biodivers.* 15 (5) <https://doi.org/10.1002/cbdv.201700567>.
- Choi, S., Nguyen, V.T., Tae, N., Lee, S., Ryou, S., Min, B.S., Lee, J.H., 2014. Anti-inflammatory and heme oxygenase-1 inducing activities of lanostane triterpenes isolated from mushroom Ganoderma lucidum in RAW264.7 cells. *Toxicol. Appl. Pharmacol.* 280 (3) <https://doi.org/10.1016/j.taap.2014.09.007>.
- Chung, D.J., Yang, M.Y., Li, Y.R., Chen, W.J., Hung, C.Y., Wang, C.J., 2017. Ganoderma lucidum repress injury of ethanol-induced steatohepatitis via anti-inflammation, anti-oxidation and reducing hepatic lipid in C57BL/6J mice. *J. Funct. Foods* 33. <https://doi.org/10.1016/j.jff.2017.03.059>.

- Dragomanova, S., Miteva, S., Nicoletti, F., Mangano, K., Fagone, P., Pricoco, S., Staykov, H., Tancheva, L., 2021. Therapeutic potential of alpha-lipoic acid in viral infections, including COVID-19. *Antioxidants* 10 (Issue 8). <https://doi.org/10.3390/antiox10081294>.
- Dudhgaonkar, S., Thyagarajan, A., Sliva, D., 2009. Suppression of the inflammatory response by triterpenes isolated from the mushroom Ganoderma lucidum. *Int. Immunopharm.* 9 (11) <https://doi.org/10.1016/j.intimp.2009.07.011>.
- Feng, X., Wang, Y., 2019. Anti-inflammatory, anti-nociceptive and sedative-hypnotic activities of lucidone D extracted from Ganoderma lucidum. *Cell. Mol. Biol.* 65 (4) <https://doi.org/10.14715/cmb/2019.65.4.6>.
- Fu, Y., Shi, L., Ding, K., 2019. Structure elucidation and anti-tumor activity in vivo of a polysaccharide from spores of Ganoderma lucidum (Fr.) Karst. *Int. J. Biol. Macromol.* 141 <https://doi.org/10.1016/j.jbiomac.2019.09.046>.
- Fujita, R., Liu, J., Shimizu, K., Konishi, F., Noda, K., Kumamoto, S., Ueda, C., Tajiri, H., Kaneko, S., Suimi, Y., Kondo, R., 2005. Anti-androgenic activities of Ganoderma lucidum. *J. Ethnopharmacol.* 102 (1) <https://doi.org/10.1016/j.jep.2005.05.041>.
- González, A., Atienza, V., Montoro, A., Soriano, J.M., 2020. Use of ganoderma lucidum (Ganodermataceae, basidiomycota) as radioprotector. *Nutrients* 12 (Issue 4). <https://doi.org/10.3390/nu12041143>.
- Gurunathan, S., Raman, J., Abd Malek, S.N., John, P.A., Vikineswary, S., 2013. Green synthesis of silver nanoparticles using Ganoderma neo-japonicum Imazeki: a potential cytotoxic agent against breast cancer cells. *Int. J. Nanomed.* 8 <https://doi.org/10.2147/IJN.S51881>.
- Ha, D.T., Oh, J., Minh Khoi, N., Dao, T.T., Dung, L.V., Do, T.N.Q., Lee, S.M., Jang, T.S., Jeong, G.S., Na, M., 2013. In vitro and in vivo hepatoprotective effect of ganodermanontriol against t-BHP-induced oxidative stress. *J. Ethnopharmacol.* 150 (3) <https://doi.org/10.1016/j.jep.2013.09.039>.
- Hetland, G., Johnson, E., Bernardshaw, S.V., Grinde, B., 2021. Can medicinal mushrooms have prophylactic or therapeutic effect against COVID-19 and its pneumonic superinfection and complicating inflammation? *Scand. J. Immunol.* 93 (Issue 1) <https://doi.org/10.1111/sji.12937>.
- Hu, Z., Du, R., Xiu, L., Bian, Z., Ma, C., Sato, N., Hattori, M., Zhang, H., Liang, Y., Yu, S., Wang, X., 2020. Protective effect of triterpenes of Ganoderma lucidum on lipopolysaccharide-induced inflammatory responses and acute liver injury. *Cytokine* 127. <https://doi.org/10.1016/j.cyto.2019.154917>.
- Jaiswal, M., LaRusso, N.F., Burgart, L.J., Gores, G.J., 2000. Inflammatory cytokines induce DNA damage and inhibit DNA repair in cholangiocarcinoma cells by a nitric oxide-dependent mechanism. *Cancer Res.* 60 (1).
- Kim, M.S., Kim, J.Y., 2017. Intestinal anti-inflammatory effects of cinnamon extracts in a co-culture model of intestinal epithelial Caco-2 cells and RAW264.7 macrophages. *Applied Biological Chemistry* 60 (5). <https://doi.org/10.1007/s13765-017-0311-y>.
- Lachowicz, S., Seliga, Ł., Pluta, S., 2020. Distribution of phytochemicals and antioxidative potency in fruit peel, flesh, and seeds of Saskatoon berry. *Food Chem.* 305 (April 2019), 125430 <https://doi.org/10.1016/j.foodchem.2019.125430>.
- Lau, M.F., Chua, K.H., Sabaratnam, V., Kuppasamy, U.R., 2022. In vitro anti-colicorectal cancer potential of the medicinal mushroom ganoderma neo-japonicum Imazeki in hyperglycemic condition: impact on oxidative stress, cell cycle and apoptosis. *Nutr. Cancer* 74 (3). <https://doi.org/10.1080/01635581.2021.1931701>.
- Lee, E.H., Cho, J.H., Kim, D.H., Hong, S.H., Kim, N.H., Park, M.J., Hong, E.J., Cho, Y.J., 2017. Anti-inflammatory activity of manassantin A from ultra-fine ground Saururus chinensis in lipopolysaccharide-stimulated RAW 264.7 cells. *Applied Biological Chemistry* 60 (1). <https://doi.org/10.1007/s13765-016-0249-5>.
- Leskosk-Cukalovic, I., Despotovic, S., Lalic, N., Niksic, M., Nedovic, V., Tesovic, V., 2010. Ganoderma lucidum - medicinal mushroom as a raw material for beer with enhanced functional properties. *Food Res. Int.* 43 (9) <https://doi.org/10.1016/j.foodres.2010.07.014>.
- Lin, J.M., Lin, C.C., Chen, M.F., Ujiie, T., Takada, A., 1995. Radical scavenger and antihepatotoxic activity of Ganoderma formosanum, Ganoderma lucidum and Ganoderma neo-japonicum. *J. Ethnopharmacol.* 47 (1) [https://doi.org/10.1016/0378-8741\(95\)01251-8](https://doi.org/10.1016/0378-8741(95)01251-8).
- Ling-Sing Seow, S., Naidu, M., David, P., Wong, K.H., Sabaratnam, V., 2013. Potentiation of neurotogenic activity of medicinal mushrooms in rat pheochromocytoma cells. *BMC Compl. Alternative Med.* 13 <https://doi.org/10.1186/1472-6882-13-157>.
- Liu, C., Dunkin, D., Lai, J., Song, Y., Ceballos, C., Benkov, K., Li, X.M., 2015. Anti-inflammatory effects of Ganoderma lucidum triterpenoid in human Crohn's disease associated with downregulation of NF-κB signaling. *Inflamm. Bowel Dis.* 21 (8) <https://doi.org/10.1097/MIB.0000000000000439>.
- Liu, Z., Qiu, P., Li, J., Chen, G., Chen, Y., Liu, H., She, Z., 2018. Anti-inflammatory polyketides from the mangrove-derived fungus Ascomycota sp. SK2YWS-L. *Tetrahedron* 74 (7). <https://doi.org/10.1016/j.tet.2017.12.057>.
- Loboda, A., Damulewicz, M., Pyza, E., Jozkowicz, A., Dulak, J., 2016. Role of Nrf2/HO-1 system in development, oxidative stress response and diseases: an evolutionarily conserved mechanism. *Cell. Mol. Life Sci.* 73 (Issue 17) <https://doi.org/10.1007/s00018-016-2223-0>.
- Ma, K., Ren, J., Han, J., Bao, L., Li, L., Yao, Y., Sun, C., Zhou, B., Liu, H., 2014. Ganoboninketals A-C, antiplasmodial 3,4-seco-27-norlanostane triterpenes from Ganoderma boninense Pat. *J. Nat. Prod.* 77 (8) <https://doi.org/10.1021/np5002863>.
- Maheshwari, S., Kumar, V., Bhaduria, G., Mishra, A., 2022. Immunomodulatory potential of phytochemicals and other bioactive compounds of fruits: a review. *Food Frontiers* 3 (2), 221–238. <https://doi.org/10.1002/fft2.129>.
- Martínez-Montemayor, M.M., Ling, T., Suárez-Arroyo, L.J., Ortiz-Soto, G., Santiago-Negrón, C.L., Lacourt-Ventura, M.Y., Valentín-Acevedo, A., Lang, W.H., Rivas, F., 2019. Identification of biologically active ganoderma lucidum compounds and synthesis of improved derivatives that confer anti-cancer activities in vitro. *Front. Pharmacol.* 10 (FEB) <https://doi.org/10.3389/fphar.2019.00115>.

- Mi, X., Zeng, G.R., Liu, J.Q., Luo, Z.S., Zhang, L., Dai, X.M., Fang, W.T., Zhang, J., Chen, X.C., 2022. Ganoderma lucidum triterpenoids improve maternal separation-induced anxiety-and depression-like behaviors in mice by mitigating inflammation in the periphery and brain. *Nutrients* 14 (11). <https://doi.org/10.3390/nu14112268>.
- Natoli, G., Chiocca, S., 2008. Nuclear ubiquitin ligases, NF- $\kappa$ B degradation, and the control of inflammation. *Sci. Signal.* 1 (1) <https://doi.org/10.1126/stke.11pe1>.
- Obrenovich, M.E., Li, Y., Parvathaneni, K., Yendluri, B., Palacios, H., Leszek, J., Aliev, G., 2012. Antioxidants in health, disease and aging. *CNS Neurol. Disord. - Drug Targets* 10 (2). <https://doi.org/10.2174/187152711794480375>.
- Pan, Y., Yuan, S., Teng, Y., Zhang, Z., He, Y., Zhang, Y., Liang, H., Wu, X., Li, J., Yang, H., Zhou, P., 2022. Antioxidation of a proteoglycan from Ganoderma lucidum protects pancreatic  $\beta$ -cells against oxidative stress-induced apoptosis in vitro and in vivo. *Int. J. Biol. Macromol.* 200 <https://doi.org/10.1016/j.ijbiomac.2022.01.044>.
- Park, J., Min, J.S., Kim, B., Chae, U. Bin, Yun, J.W., Choi, M.S., Kong, I.K., Chang, K.T., Lee, D.S., 2015. Mitochondrial ROS govern the LPS-induced pro-inflammatory response in microglia cells by regulating MAPK and NF- $\kappa$ B pathways. *Neurosci. Lett.* 584 <https://doi.org/10.1016/j.neulet.2014.10.016>.
- Peng, Z., Hu, X., Li, X., Jiang, X., Deng, L., Hu, Y., Bai, W., 2020. Protective effects of cyanidin-3-O-glucoside on UVB-induced chronic skin photodamage in mice via alleviating oxidative damage and anti-inflammation. *Food Frontiers* 1 (3), 213–223. <https://doi.org/10.1002/fft2.26>.
- Platnich, J.M., Chung, H., Lau, A., Sandall, C.F., Bondzi-Simpson, A., Chen, H.M., Komada, T., Trotman-Grant, A.C., Brandelli, J.R., Chun, J., Beck, P.L., Philpott, D.J., Girardin, S.E., Ho, M., Johnson, R.P., MacDonald, J.A., Armstrong, G.D., Muruve, D. A., 2018. Shiga toxin/lipopolysaccharide activates caspase-4 and gasdermin D to trigger mitochondrial reactive oxygen species upstream of the NLRP3 inflammasome. *Cell Rep.* 25 (6) <https://doi.org/10.1016/j.celrep.2018.09.071>.
- Qiu, J., Wang, X., Song, C., 2016. Neuroprotective and antioxidant lanostanoid triterpenes from the fruiting bodies of Ganoderma atrum. *Fitoterapia* 109. <https://doi.org/10.1016/j.fitote.2015.12.008>.
- Shao, G., He, J., Meng, J., Ma, A., Geng, X., Zhang, S., Qiu, Z., Lin, D., Li, M., Zhou, H., Lin, S., Yang, B., 2021. Ganoderic acids prevent renal ischemia reperfusion injury by inhibiting inflammation and apoptosis. *Int. J. Mol. Sci.* 22 (19) <https://doi.org/10.3390/ijms221910229>.
- Sheng, F., Zhang, L., Wang, S., Yang, L., Li, P., 2020. Deacetyl ganoderic acid F inhibits LPS-induced neural inflammation via NF- $\kappa$ B pathway both in vitro and in vivo. *Nutrients* 12 (1). <https://doi.org/10.3390/nu12010085>.
- Smina, T.P., De, S., Devasagayam, T.P.A., Adhikari, S., Janardhanan, K.K., 2011a. Ganoderma lucidum total triterpenes prevent radiation-induced DNA damage and apoptosis in splenic lymphocytes in vitro. *Mutat. Res., Genet. Toxicol. Environ. Mutagen.* 726 (2) <https://doi.org/10.1016/j.mrgentox.2011.09.005>.
- Smina, T.P., Mathew, J., Janardhanan, K.K., Devasagayam, T.P.A., 2011b. Antioxidant activity and toxicity profile of total triterpenes isolated from Ganoderma lucidum (Fr.) P. Karst occurring in South India. *Environ. Toxicol. Pharmacol.* 32 (3) <https://doi.org/10.1016/j.etap.2011.08.011>.
- Su, H.G., Peng, X.R., Shi, Q.Q., Huang, Y.J., Zhou, L., Qiu, M.H., 2020. Lanostane triterpenoids with anti-inflammatory activities from Ganoderma lucidum. *Phytochemistry* 173. <https://doi.org/10.1016/j.phytochem.2019.112256>.
- Subramaniam, S., Sabaratnam, V., Kuppusamy, U.R., 2015. Solid-substrate fermentation of wheat grains by mycelia of indigenous Ganoderma spp. enhanced adipogenesis and modulated PPAR $\gamma$  expression in 3T3-L1 cells. *Chiang Mai J. Sci.* 42 (2).
- Tak, P.P., Firestein, G.S., 2001. NF- $\kappa$ B: a key role in inflammatory diseases. *J. Clin. Invest.* 107 (1), 7–11. <https://doi.org/10.1172/JCI11830>.
- Wang, C., Choi, Y.H., Xian, Z., Zheng, M., Piao, H., Yan, G., 2018. Aloperine suppresses allergic airway inflammation through NF- $\kappa$ B, MAPK, and Nrf2/HO-1 signaling pathways in mice. *Int. Immunopharm.* 65 <https://doi.org/10.1016/j.intimp.2018.11.003>.
- Wei, Z.H., Chen, N., Li, Y.J., Fan, Q.L., Yu, T.F., Wang, K.X., Dong, B.T., Fan, E.Y., Yuan, P.L., Hu, G.W., Qiao, F., Ge, L., Deng, Y.Y., Lv, Y. ning, Hu, B. feng, Liu, L., 2018. Glucose fed-batch integrated dissolved oxygen control strategy enhanced polysaccharide, total triterpenoids and inotodiol production in fermentation of a newly isolated Inonotus obliquus strain. *Process Biochem.* 66 <https://doi.org/10.1016/j.procbio.2018.01.006>.
- Wu, Y.L., Han, F., Luan, S.S., Ai, R., Zhang, P., Li, H., Chen, L.X., 2019. Triterpenoids from ganoderma lucidum and their potential anti-inflammatory effects. *J. Agric. Food Chem.* 67 (18) <https://doi.org/10.1021/acs.jafc.9b01195>.
- Xing, J.H., Sun, Y.F., Han, Y.L., Cui, B.K., Dai, Y.C., 2018. Morphological and molecular identification of two new Ganoderma species on Casuarina equisetifolia from China. *MycKeys* 34. <https://doi.org/10.3897/mycokeys.34.22593>.
- Xu, J., Xiao, C.M., Xu, H.S., Yang, S.X., Chen, Z.M., Wang, H.Z., Zheng, B.S., Mao, B.Z., Wu, X.Q., 2021. Anti-inflammatory effects of Ganoderma lucidum sterols via attenuation of the p38 MAPK and NF- $\kappa$ B pathways in LPS-induced RAW 264.7 macrophages. *Food Chem. Toxicol.* 150 <https://doi.org/10.1016/j.fct.2021.112073>.
- Xue, Q., Yan, Y., Zhang, R., Xiong, H., 2018. Regulation of iNOS on immune cells and its role in diseases. *Int. J. Mol. Sci.* 19 (Issue 12) <https://doi.org/10.3390/ijms19123805>.
- Yamamoto, M., Kensler, T.W., Motohashi, H., 2018. The KEAP1-NRF2 system: a thiol-based sensor-effector apparatus for maintaining redox homeostasis. *Physiol. Rev.* 98 (Issue 3) <https://doi.org/10.1152/physrev.00023.2017>.
- Yu, N., Huang, Y., Jiang, Y., Zou, L., Liu, X., Liu, S., Chen, F., Luo, J., Zhu, Y., 2020. Ganoderma lucidum triterpenoids (GLTs) reduce neuronal apoptosis via inhibition of ROCK signal pathway in APP/PS1 transgenic alzheimer's disease mice. *Oxid. Med. Cell. Longev.* <https://doi.org/10.1155/2020/9894037>, 2020.
- Yuan, H., Xu, Y., Luo, Y., Zhang, J.R., Zhu, X.X., Xiao, J.H., 2022. Ganoderic acid D prevents oxidative stress-induced senescence by targeting 14-3-3 $\epsilon$  to activate CaM/CaMKII/NRF2 signaling pathway in mesenchymal stem cells. *Aging Cell* 21 (9), 1–19. <https://doi.org/10.1111/acer.13686>.
- Zeng, Q., Zhou, F., Lei, L., Chen, J., Lu, J., Zhou, J., Cao, K., Gao, L., Xia, F., Ding, S., Huang, L., Xiang, H., Wang, J., Xiao, Y., Xiao, R., Huang, J., 2017. Ganoderma lucidum polysaccharides protect fibroblasts against UVB-induced photoaging. *Mol. Med. Rep.* 15 (1) <https://doi.org/10.3892/mmr.2016.6026>.
- Zhang, D.D., Chapman, E., 2020. The role of natural products in revealing NRF2 function. *Nat. Prod. Rep.* 37 (Issue 6) <https://doi.org/10.1039/c9np00061e>.
- Zhang, X.D., Li, Z., Liu, G.Z., Wang, X., Kwon, O.K., Lee, H.K., Whang, W.K., Liu, X.Q., 2016. Quantitative determination of 15 bioactive triterpenoid saponins in different parts of Acanthopanax henryi by HPLC with charged aerosol detection and confirmation by LC-ESI-TOF-MS. *J. Separ. Sci.* 39 (12) <https://doi.org/10.1002/jssc.201501029>.
- Zhang, Y., Wang, X., Yang, X., Yang, X., Xue, J., Yang, Y., 2021. Ganoderic acid A to alleviate neuroinflammation of alzheimer's disease in mice by regulating the imbalance of the Th17/tregs Axis. *J. Agric. Food Chem.* 69 (47) <https://doi.org/10.1021/acs.jafc.1c06304>.
- Zheng, Shizhong, Zhang, W., Liu, S., 2020. Optimization of ultrasonic-assisted extraction of polysaccharides and triterpenoids from the medicinal mushroom Ganoderma lucidum and evaluation of their in vitro antioxidant capacities. *PLoS One* 15 (12 December). <https://doi.org/10.1371/journal.pone.0244749>.
- Zheng, Sihua, Ma, J., Zhao, X., Yu, X., Ma, Y., 2022. Ganoderic acid A attenuates IL-1 $\beta$ -induced inflammation in human nucleus pulposus cells through inhibiting the NF- $\kappa$ B pathway. *Inflammation* 45 (2). <https://doi.org/10.1007/s10753-021-01590-0>.